A Multi-Rocket Piston Model to Study Three-Dimensional Asymmetries in Implosions at the National Ignition Facility

D T. Casey, [1] J. Kunimune[2], O. A. Hurricane,[1,] O L. Landen, [1] P. Springer,[1] R. M. Bionta,[1] C. V. Young,[1] R. C. Nora, B. J. MacGowan,[1] J. A. Gaffney, [1] B. Kustowski, [1] C. Weber, [1] A. Kritcher, [1] J. Milovich, [1] S. Haan ,[1] M. Gatu Johnson[2] , D. Schlossberg, [1] S. Kerr, [1] P. L. Volegov, [1] D. N. Fittinghoff, [1] V. Geppert-Kleinrath,[3] C. H. Wilde, [3] M. Freeman [3]

[1]*Lawrence Livermore National Laboratory, Livermore, CA 94550*

[2]*Massachusetts Institute of Technology, Cambridge, MA 02139*

[3] *Los Alamos National Laboratory, Los Alamos, NM 87545*

Ignition and gain greater than unity has been achieved in inertial confinement fusion (ICF) implosions at the National Ignition Facility (NIF). These accomplishments required implosions that produced high hotspot pressures that are inertially confined by a dense shell of DT fuel. However, even in the burning and igniting plasma regime, 3D asymmetries can reduce the coupling of shell kinetic energy to the hotspot harming the overall implosion performance and truncating burn. Likewise, the overall scale of the implosion can be minimized by maintaining a high efficiency of energy coupling from the imploding shell to the hotspot. Recent experiments commonly show signs of significant 3D asymmetry that manifest as high hotspot velocity or asymmetry in the self-emission and scattered neutron images. While modeling 3D asymmetries in implosion with full scale hydrodynamic simulations is often performed, it is labor intensive and computationally costly. Therefore, 3D simulation is applied only in special cases like experiments of particular interest. To enable a wider survey of 3D post-shot analysis, an approximate but computationally inexpensive approach is applied by using multiple rocket-pistons discretizing the spherical implosion. These rocket-pistons are coupled together through the central hotspot pressure using the power balance equations. The approach is similar to that reported by Springer [Springer et al., Nuclear Fusion **59** (3) (2019)] with the inclusion of an approximate hohlraum model beginning at the rocket-implosion stage and post-processing of realistic synthetic diagnostic data at the stagnation and peak burn. This rocket piston tool can provide approximate 3D image and diagnostic data that can then be compared quantitively with data enabling new techniques in iterative, forward fitting, and machine learning to interpreting measurements.

I. Introduction

Lawson's criterion for ignition was exceeded[1] in experiments at the National Ignition Facility (NIF)[2] and gain greater than unity demonstrated.[3] In these experiments, capsules filled with deuterium and tritium fuel are imploded to high enough densities and temperatures to initiate alpha-particle self-heating and fusion burn.[4, 5] Using "indirect drive," a laser irradiates the interior of a high-Z (Au lined depleted uranium) cylindrical hohlraum, which produces a nearly uniform, thermal, x-ray drive. The x-rays then heat and ablate an outer capsule shell, imploding the remaining cryogenically frozen DT shell-mass inward. This imploding shell then stagnates on a lower density DT gas to form a hotspot. The pressure P (or energy density) and temperature of the hotspot enable fusion reactions to occur. To ignite the hotspot and surrounding fuel, the hotspot P must be confined for a sufficient time τ to enable a burn-wave through the dense DT shell. This requirement can also be expressed as a requirement on the product of hotspot $P\tau$[6, 7] and the hotspot temperature. To produce high $P\tau$, at the relevant temperatures, an implosion must have high in-flight implosion velocity (v_{imp}), efficient coupling between the inflight shell and hotspot, and high $\int \rho dr$ or areal-density (ρR) at stagnation.

Asymmetries in the imploded ρR reduce the coupling of the shell kinetic energy and the confinement of the hotspot pressure. In prior work,[8] it was shown that the residual kinetic energy (RKE, normalized to shell kinetic energy) due to a mode-1 asymmetry (e.g. top/down) is related to a metric of the ρR asymmetry, $f = \frac{\rho R_{max} - \rho R_{min}}{\rho R_{max} + \rho R_{min}} \approx \frac{v_{HS}}{v_{imp}}$, where ρR_{max} and ρR_{min} are the maximum and minimum areal-densities of the dense shell, respectively; v_{HS} is the bulk velocity of the burning hotspot[9] near peak convergence, and v_{imp} is the peak implosion velocity. With $f^2 \approx RKE$, The Lawson parameter and yield are degraded by $\frac{P\tau}{P\tau_{1D}} \approx (1 - f^2)$ and $\frac{Y}{Y_{1D}} \approx (1 - f^2)^{10/3}$ in the limit of no alpha-heating feedback. Further work[8, 10, 11] treating higher mode and 3D asymmetries, showed that equivalently $f^2 = 1 - \rho R_{WHM}/\rho R_{AVG}$ where ρR_{WHM} and ρR_{AVG} are the weighted harmonic mean and average areal densities, respectively. However, determining the $\rho R_{WHM}/\rho R_{AVG}$ with the available instrumentation on the NIF is extremely challenging, especially in the presence of 3D asymmetries which can manifest in each of the limited diagnostic line-of-sights in complicated ways. Empirical observations from NIF have shown that scattered-neutron images work well to constrain the $\rho R_{WHM}/\rho R_{AVG}$ when the implosion is well approximated by 2D symmetry, but that strong 3D asymmetries induced by mode-1 make the inference of $\rho R_{WHM}/\rho R_{AVG}$ difficult because one or more of the images becomes dominated by features whose modal content requires more lines-of sight than available to resolve. Likewise, theoretical and computational analysis of direct-drive implosions at OMEGA have come to similar conclusions and faced similar limited diagnostic challenges.[12-14]

Nevertheless, to better understand the performance of ICF implosion experiments, diagnosing the symmetry of the stagnated fuel is extremely important. ICF implosions produce copious numbers of 14 MeV D+T neutrons. Therefore, imaging of the primary hotspot region that emits these neutrons is possible using the neutron imaging systems (NIS),[15-17] and a range of tomographic reconstruction techniques have been developed for the hotspot symmetry.[17] However, measurements of the symmetry of the dense shell are indirect and typically involve secondary scattering processes. The most common techniques include down-scattered neutron images,[15-17] neutron time of flight (nTOF)[18-20] and magnetic recoil spectrometry (MRS)[21] measurements of scattered neutrons, and real-time neutron activation detectors (RTNADs)[22] of attenuated primary 14 MeV neutrons as they traverse the dense shell. Ideally, a full reconstruction of the

implosion symmetry would combine all available data but because these measures of asymmetry are based on different principles that is challenging. A solution is to develop a model that can do this and fully leverage the 3D information contained in the neutron images, the RTNADs, and neutron spectral measurements of the down-scatter ratio and the measured hotspot velocity.

This paper will describe a numerical rocket-piston model developed to be a computational inexpensive alternative tool for modeling 3D asymmetry in ICF experiments at the NIF and to enable 3D reconstructions with multiple disparate sets of data. Section I of this paper introduces the subject. Section II will discuss the components of the model and how they are integrated into a 3D calculation with synthetic diagnostic data. Section III will apply the model to an example high-yield ignition experiment. Finally, Section IV will put this work into context and summarize.

II. Numerical Rocket Piston model

Combining multiple pieces of diagnostic data into an integrated implosion model has been performed before in various levels of complexity. For example, an integrated model was developed by Cerjan, Springer, and Sepke [23] to perform a static 3D fit using HYDRA[24] to various diagnostic signatures, Gaffney et al.[25] developed a Bayesian inference technique to combine X-ray and neutron data, Nora et al.[26] used Gaussian process regress to interpolate through a set of a few thousand 3D HYDRA capsule-only simulations, and Springer et al.[27] split the implosion into multiple facets that were initialized at peak-velocity and then coupled through the hotspot alpha-power balance equations. The development of the current rocket piston model was motivated on the following features that were found in most of the previous implementations but not all together in one model. First, it was desired that the model be extremely fast, computationally inexpensive, and yet scalable for ensemble calculations and to enable inversions and forward fitting techniques. Second, it was important that the model produce realistic synthetic diagnostic data that can be compared directly with experiment. Third, it was desired that the model could be executed from end-to-end, beginning with target capsule metrology and laser power balance data and ending with synthetic DT neutron diagnostic data. Fourth, simplified implosion physics models of this type provide great insight into the key physics of ICF implosions. Additionally, this model was developed to execute in a python environment to enable use with machine learning tools.

A. Hohlraum and rocket model

Similar to recent analytic models developed by Hurricane et al.,[8, 10] and numerical model of Springer et al.,[27] the implosion can be abstracted into a number of discrete segments. A comparison of a detailed 2D radiation hydrodynamics simulation and a spherical segmented implosion subjected to an ℓ=1 mode perturbation is shown in Figure 1.

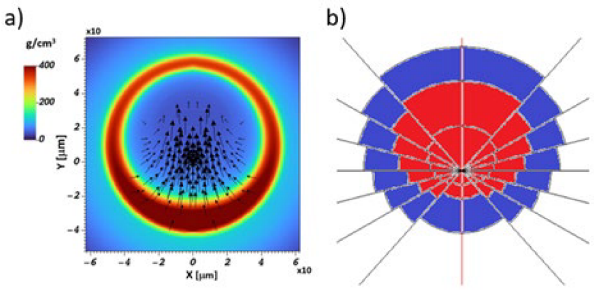

Figure 1: a) A 2D HYDRA simulation of a 1% ℓ=1 asymmetry leading to a ρR asymmetry and bulk flow. b) A segmented approximation of the ℓ =1 asymmetry using the rocket-piston model.

This model will begin at t=0 and attempt to approximate the growth of low-mode dynamics throughout the implosion given an initial perturbation of the shell thickness or mass (one of the principal causes for low-mode asymmetry in ignition experiments[28]). The shell represents the DT fuel and ablator material. Under the assumption of an incompressible and thin shell (Δ<<R), we can write the equations of motion in spherical geometry using Newton's law (or the "rocket-equations")[29, 30] for each piston segment as:

$$\dot{m} = -4\pi R^2 m_a$$

$$m \ddot{R} = -4\pi R^2 (p_a - p_{HS}) \quad (1)$$

where m is the segment mass, m_a is the mass ablation rate, p_a is the ablation pressure, R is the spherical radius and p_{hs} is the hotspot pressure (discussed in the next section). The m_a and p_a are determined using the fits by Olson et al.[29] Note that here we have neglected the mass ablation fo the dense shell into the hotspot which is justifyable because typically $m_{hs} << m_{shell}$ but it is also easily including by adding another mass ablation term.[31] Note also that the segment solid angle appears on both left and right sides of each equation but has been dropped here for simplicity because they are assumed to be equal and constant throughout the implosion. These equations of motions can be repeated for arbitrary number of shell segments with equal solid angle, or rocket-pistons, and are coupled through the shared central hotspot pressure. The shell mass, m, is assumed to be related to the initial shell mass times of each piston and an adjustable multiplier (~0.67) that approximately accounts for compressibilty of each piston (neglecting the dynamics). A dynamic model[27] for the compressibility by treating an outgoing shock has been encorperated as well but is not discussed further here.

To estimate the x-ray radiation drive from hohlraum geometry and delivered laser pulse shape we use an approximate hohlraum model developed by Callahan et al..[32] The result of the estimated radiation drive for shot N210207 is shown in Figure 2 compared to the measured pulse shape and the DANTE[33, 34] radiation temperature. The model drive gets close to the DANTE result, but in order to match the implosion bangtime, an overall scalar drive multiplier on the flux was applied. To solve the equations of motion, we can approximate the hotspot pressure by assuming an adiabatic hotspot, or pV^{γ} = const, and adjusting the stagnation pressure at minimum volume by adjusting the initial pressure. Assuming pV^{γ} = const is not a requirement when introducing the

hotspot power balance equations, as discussed in the next section, but is done so here for simplicity and well approximates the power balance equations for mid 10^{16} yields when alpha heating and bremsstrahlung levels are comparable.[35] A comparison of the full radius vs time trajectory for a 1D implosion (with no initial asymmetry) is plotted in Figure 2b and compared to 1D HYDRA post-shot simulations. Also shown is the hotspot pressure.

It is important to note that in solving Eq. 1 it was assumed that there is only radial mass flow, and therefore the effects of the Rayleigh-Taylor (RT) instability were neglected. The effects of lateral flow induced by the RT instability can be important in the acceleration phase, particularly for ℓ>>1, that can develop into ρR asymmetries and those effects are currently neglected here. Nevertheless, the dynamics near stagnation have been shown in prior work[27, 36] to be mostly dominated by radial flow for low mode asymmetries. ρR asymmetries that were caused by earlier-time lateral flows may themselves induce asymmetries in radial flow due to asymmetry in confinement resulting. However, we assume here (as in prior work)[27] that the stagnation dynamics are dominated by mostly radial flow.

To help understand the impact of neglecting lateral flow, we can examine the results for a detailed 2D HYDRA simulation. In particular, a post-shot simulation of N221204[3] (Y=3.1 MJ) that approximately matches the measured symmetry using a dynamic swinging P2 in the drive. Figure 2 shows the resultant radial (KE_{rad}) and non-radial kinetic energy (KE_{rot}) as a function of time between peak velocity and bangtime. Note that minimum volume (also approximately the point of minimum radial kinetic energy) occurs ~50 ps before bang-time because this burning simulation extends into the expansion phase. The results show that the initial P2 asymmetry may induce ρR asymmetries early in time, in part due to lateral flow, but that later in time the kinetic energy of the flow is dominated by radial motion, where the contribution of non-radial flow is ~10% of the total. Therefore, a model that reproduces stagnation ρR asymmetries is expected to reasonably describe the dynamics of low-mode asymmetries.

In future work, inclusion of non-radial flows may be possible in this framework, as shown by Amendt et. al.[30] Nevertheless, the results neglecting lateral flow should still be useful in reconstructing the stagnation profiles to match data.

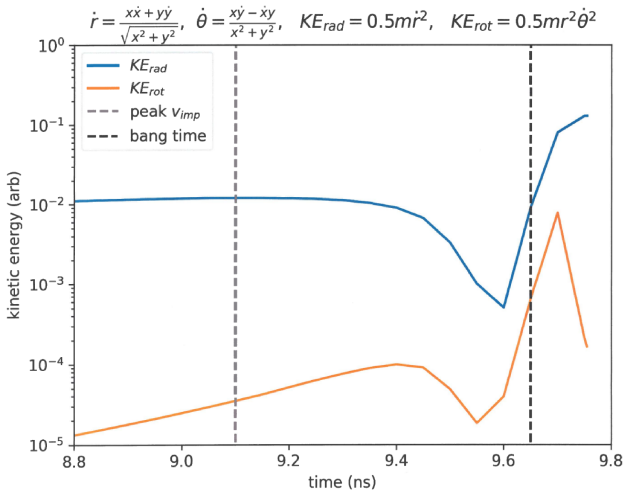

Figure 2: 2D HYDRA simulation of shot N221204 with a dynamic P2 swing (drive includes a time dependent dP2/dt) that approximately matches observations. The plot shows the radial flow kinetic energy (blue curve) and the rotational flow kinetic energy (orange curve) as a function of time around peak velocity (grey dashed line) and bangtime (black line).

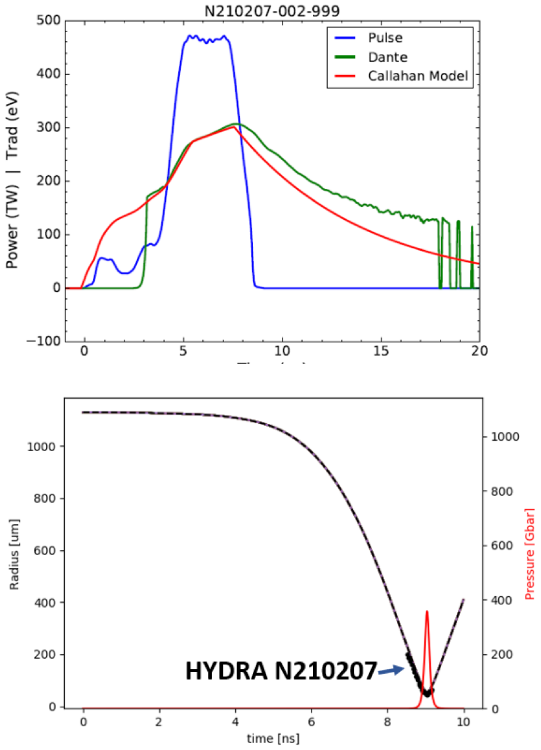

Figure 3: a) Measured laser pulse shape, DANTE measured radiation temperature, and Callahan model radiation temperature for shot N210207. The radiation drive calculated from the Callahan model is used to ablate the rocket-pistons. b) Radius versus time for a rocket-piston calculation of N210207 using radiation drive calculated in part 'a' but adjusted to match the measured bangtime compared to 1D HYDRA simulations. Also shown is the pressure from the rocket-piston calculation assuming an adiabat hotspot.

B. Multi-piston model coupled with fusion power balance

The hotspot pressure in Equation 1 can be calculating using the fusion power balance equations discussed by Hurricane[31] and Springer et al.[27] and coupled to the equations of motion (note that in Hurricane the Q's in Eq. (2) are power per unit hotspot mass while in Springer, the Q's are power as adopted here). More specifically, the hotspot p_{HS} and temperature (T_{hs}) equations are:

$$\frac{dp_{HS}}{dt} = \frac{p_{HS}}{E_{HS}}\left(Q_a - Q_{rad} - \frac{5}{2}p_{HS}\frac{dV}{dt}\right)$$
$$\frac{dT_{HS}}{dt} = \frac{T_{HS}}{E_{HS}}\left(f_a Q_a - Q_{rad} - Q_{cond} - p_{HS}\frac{dV}{dt}\right) \qquad (2)$$

Here, E_{hs} is the hotspot energy, Q_a is the alpha power, Q_{rad} is the radiation loss power, Q_{cond} is the conduction loss power, and V is the volume. As in Eq. 1, p_{HS} is the central hotspot pressure (assuming an isobaric hotspot) and is the term that couples the equations of motion for each rocket-piston together. To solve the equations an initial pressure and temperature must be assumed at t=0, which are assumed to be free parameters used to adjust the pressure and temperature at bang-time (peak DT reaction rate or Qa). By disabling the radiation and alpha heating terms, one recovers the pV^{γ} = const solution shown in Figure 3b as expected.[35] The terms resulting from solving the power balance equations numerically, shown in Eq. 2 (and coupled with Eq. 1), are shown in Figure 4 for an implosion with a yield of $5x10^{16}$ and an implosion with a yield of $4x10^{18}$. In both cases we see that the bangtime occurs after minimum volume because the alpha power dominates radiation and conduction at minimum volume causing the temperature to continue climbing, or $dT/dt>0$. Note that only in the second case is $d^2T/dt^2>0$, a thermonuclear instability ignition criterion discussed by Springer.[27] The dynamics of burn after minimum volume into the expansion phase are important for the impact of low-mode asymmetries on the decompression and eventual truncation of the burn through enhanced pdV losses.

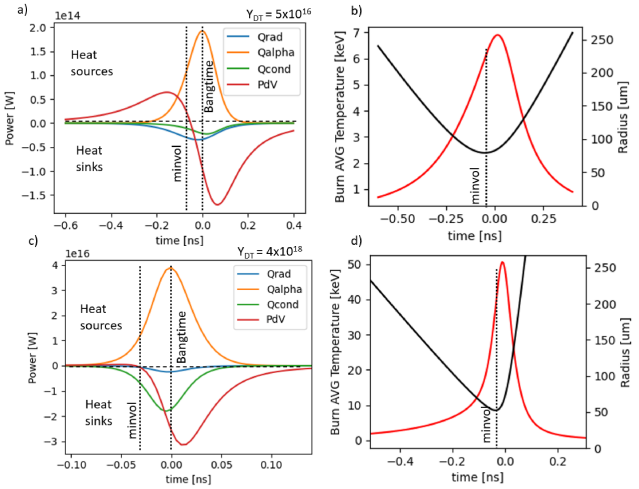

Figure 4: Power balance terms from Eq. 2 for an implosion that produces a yield of $5x10^{16}$ (a) and $4x10^{18}$ (c). Temperature versus time (red curve) and radius versus time (black curve) for an implosion that produces a yield of $5x10^{16}$ (b) and $4x10^{18}$ (d). The time in each panel is plotted relative to bangtime defined as the time of peak alpha heating power (Qa).

C. Synthetic diagnostic post-processing with MCNP

The initial capsule often has imperfections and perturbations from sphericity. The model described in the prior section can be perturbed in three dimensions by assuming that each individual capsule segment or piston has a different initial mass. For example, by initializing each segment with a perturbed mass that is described by a ℓ=1 asymmetry aligned with the Z axis or (Legendre mode P1) of 1% (peak-to-valley 2%), we get the imploded configuration shown earlier in Figure 3b. By assuming a thin, but finite thickness, incompressible shell with no lateral mass flow, we can invert the volume using the solution for the radius to estimate the areal density of each segment or $\rho\Delta_i = m/\left(4\pi R_i^2 + \frac{\pi}{3}\Delta^2\right)$. The result is shown in Figure 5a. Δ can be treated as a free parameter, calculated from the inflight and hotspot adiabats[37] or extracted from a dynamic outgoing shock model.[27]

To produce signatures that can be compared directly to imaging data, the resulting hotspot burn can be projected to produce synthetic images assuming negligibly low optical depth. However, to compare to a wider range of available diagnostic data

like the down-scattered neutron images, down-scatter ratios (DSRs), and RTNADs, the resulting piston solution and assumed profiles at bang-time can be dumped to a 3D MCNP[38] deck for postprocessing of the geometry with realistic neutron transport. The result is tallied up in ~100 small segments around the chamber sky and in three neutron imager locations according to their actual NIF chamber locations. The configuration illustrated in configuration shown earlier in Figure 1b is an output from the MCNP visual editor of the cell configurations for the 1% P1 example where red cells are hotspot zones (an arbitrary number is allowed but here there are two per piston) and blue are shell zones. The density and emissivity of the hotspot zones are calculated assuming a conduction limited profile.[27] The DSRs determined from the MCNP postprocessing of the 1% P1 example are shown in Figure 5b. As expected for a P1 and the $\rho\Delta_i$ in part a, the DSR varies from small ~ 1.8% (red) to large ~3.6% (blue) with a 4π solid angle average of 2.6%. The neutron scattered of 14 MeV neutrons off fuel and shell materials is also performed and the neutron image tallies are gated to be the same as the gates used on the NIF. The simulated fluence compensated down-scattered neutron image[16, 39] for the 1% P1 is shown in Figure 5c. Likewise, the yield / yield_avg across the chamber sky equivalent to the RTNAD data is shown in Figure 5d. The synthetic fluence compensated image and RTNAD data are also consistent with expectation for a 1% P1.

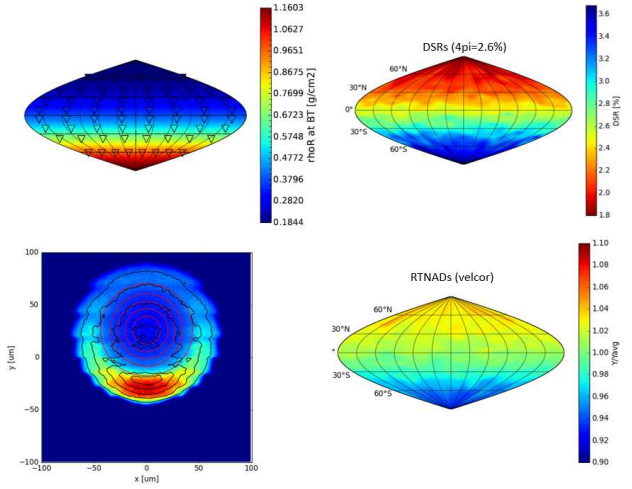

Figure 5: Synthetic diagnostics for a l=1 rocket-piston calculation that produces a ρR asymmetry shown in (a). Down-scattered ratios (b) and RTNADs relative yields (d) around the implosion sky plotted as a function of theta/phi. c) Fluence compensated down-scattered neutron image.

Given the approximations of the rocket-piston model it is interesting to compare the synthetic diagnostic results to detailed 2D HYDRA calculations of a similar implosion that gets to a similar level of asymmetry. Figure 7 shows fluence compensated image from a 2D HYDRA simulation of N170827[40] (a) and a rocket-piston calculation (b) that have imposed l=1 asymmetry of a similar magnitude. Likewise, Figure 7 has fluence compensated images from HYDRA (c) and the rocket-piston model (d) of a l=2 asymmetry.

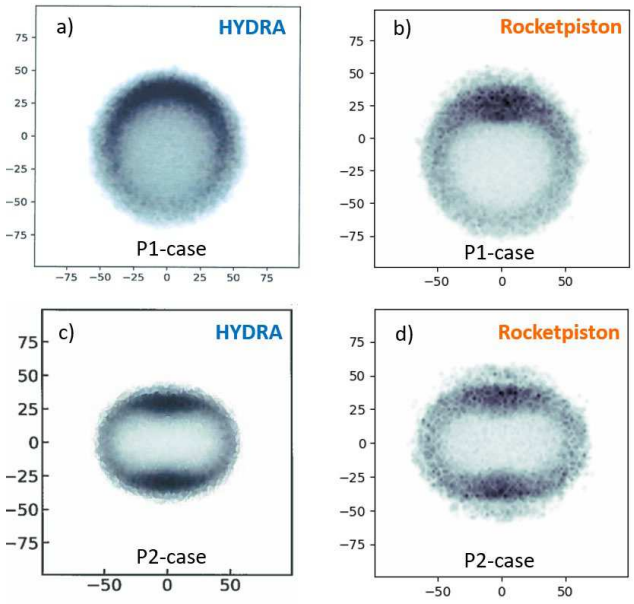

Figure 6: Fluence compensated down scattered images calculated from 2D HYDRA simulations[24] and the rocket-piston model postprocessed with MCNP.[38]

To compare more synthetic diagnostics over a range of ℓ=1 amplitudes, Figure 7 shows the yield from 2D HYDRA simulations of N170827 and rocket piston calculations versus a range of moderate to several ℓ =1 perturbations. In Figure 7a the x-axis shows the Legendre P1 amplitude of the RTNAD activation sky of 4π and Figure 7b shows the Legendre P1 amplitude of the DSR sky. The comparison shows that the rocket-piston model captures the observable to impact relationship predicted by HYDRA well. Likewise, Figure 7c and Figure 7c shows the calculated yield versus hotspot projected image P2/P0 (estimated at the 17% contour) very similar to the comparison made by Springer et al.[27] and showing similar agreement. Figure 7d shows the yield versus fluence compensated P2/P0 extracted from the integral of the fluence compensated image (as defined in reference [41]). One interesting difference appears for fluence compensated P2/P0 ~ -0.3 (very prolate with higher ρR at the equator) and may be due to saturation into higher modes from lateral flows not treated in the rocket-piston model. Outside these very prolate cases, the agreement again shows that the rocket-piston model captures the impact to observable relationship for P2.

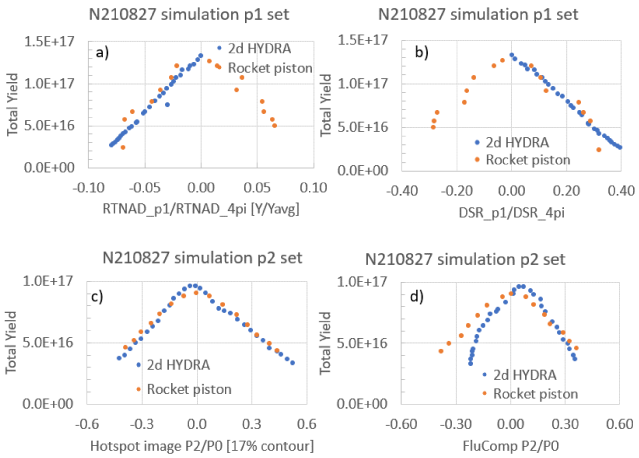

Figure 7: Total yield as a function of RTNAD p1 (a), DSR p1 (b), hotspot P2/P0 (c) and fluence compensated down-scattered image (d) for a range of initial p1 amplitudes (a,b) and p2 amplitudes (c,d).

The hotspot velocity (V_{HS}) is measured using the Doppler shifted DT-neutron spectrum[18, 42] and is a sensitive indicator of the overall ℓ =1 implosion asymmetry. The V_{HS} simulated using HYDRA is compared to two methods of estimating a flow velocity from the rocket-piston model: a calculation of the center of mass velocity of each piston at bangtime (V_{CM}) and a calculation of the velocity of the centroid of the hotspot/shell boundary determined by a spherical harmonic fit to that surface. For this set, the 2D HYDRA simulations track the centroid velocity closely and the V_{CM} is exactly 1/3 the velocity of the centroid at bangtime. The result is shown in Figure 8. The impact of internal hotspot flows is neglected in the rocket-piston model and it is not known how universal the agreement is under other initial conditions. This is the subject of ongoing work.

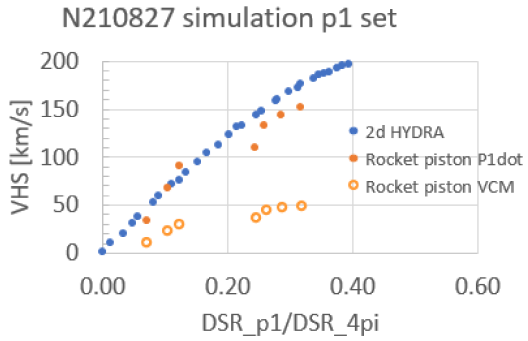

Figure 8: Calculated hotspot velocity as a function of DSR_p1/DSR_p0 (or the asymmetry metric f) using 2D HYDRA simulations, and $\dot{p}1$ and V_{CM} from the rocket-piston model.

III. Rocket piston model of N220919

Many NIF experiments show evidence of 3D asymmetries. The rocket piston model was developed to enable 3D models that could be used to study these experiments. A particular shot of interesting is N220919, a 2.05 MJ experiment that showed evidence of 2D asymmetry in the lead up to the first experiment to exceed gain > 1 (N221204).[1, 3, 43, 44] A 3D rocket piston model was used to study N220919 using ~400 rocket pistons with up to mode-4 perturbations. The initial conditions were adjusted manually until the yield, bangtime, DSR, V_{HS} and image data to provide an adequate match. There is no expectation that this solution is unique but rather illustrative of a solution consistent with most of the data and of the capabilities of this simple model to model complex 3D geometries.

To match the N220919, the initial 3D perturbation was estimated from realistic estimates of the 3D asymmetries induced by the laser power balance and target diagnostic windows calculated with a 3D view-factor model, developed by MacGowan.[45] Then the ℓ=1 component of the asymmetry was adjusted to match the observed V_{HS} direction. Next the initial drive multiplier was adjusted to match the implosion bangtime reported by the gamma-ray history (GRH) diagnostic Then initial pressure, temperature, and mass multipliers were adjust until there was an approximate match to the implosion yield, Ti and DSR determined from the nTOF[18] and MRS[46] diagnostics. The measured DSR on N220919 was 3.1% and is shown for each reported instrument line of sight in the skyplot on the chamber wall in Figure 9. The DSRs are all within uncertainty of the experiment with the exception of the 77-324 MRS DSR which is somewhat outside instrument error.

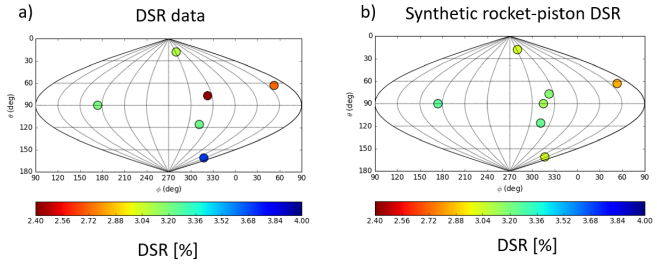

Figure 9: Comparison between measured (a) DSRs on N220919 and the synthetic (b) DSRs from the rocket-piston model.

Figure 10 shows the measured hotspot velocity on N220919 of 51 km/s toward (θ=74°,ϕ=70°) determined with the quartz Cerenkov detector (QCD) nTOF instrument.[42] The calculated center-of-mass velocity and resultant ρR distribution from the rocket-piston calculation is also shown in Figure 10. The rocket-piston velocity is 42 km/s, so 20% lower, but pointed in the same direction. Because the V_{HS} is strongly dependent on the resulting pressure and yield further adjustments are certainly possible.[47, 48] The resulting ρR

asymmetry shows contributions from ℓ=1, ℓ=2, and ℓ=3 based on the input starting assumptions and adjustments to match the V_{HS}.

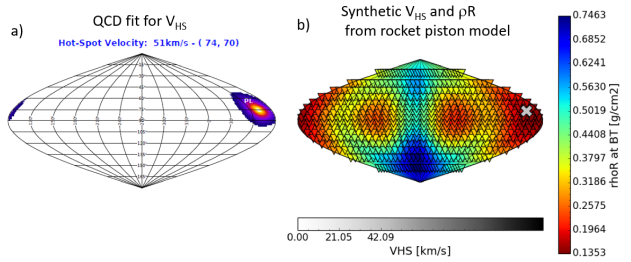

Figure 10: A comparison between the measured hotspot velocity (a) and the synthetic hotspot velocity (b) plotted as the gray 'X' overlaid with the ρR asymmetry at bang-time. The measured and calculated hotspot velocities are close in direction and magnitude.

Figure 11 shows the simulated and measured RTNAD distributions. The overall morphology of the activation between measurement and prediction is very close based on the asymmetry that came from the VF and V_{HS} adjustment.

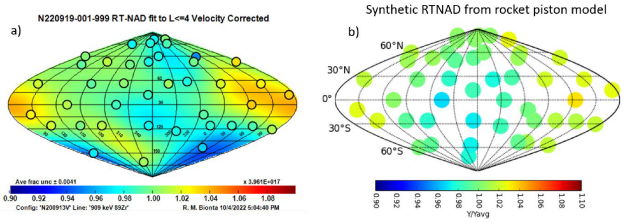

Figure 11: a) A comparison of the RTNADs relative yield measurements (a) compared to the synthetic-data (b) from the rocket piston model.

Figure 12 shows the measured fluence compensated image measured from the NIS3 diagnostic (90-213) compared to the calculated fluence compensated image. The two images both show strong ρR asymmetry resulting in high ρR 'caps' building up at the north and south pole induced by a P2 asymmetry. The data appears to be slightly stronger and the overall shape is sightly more prolate.

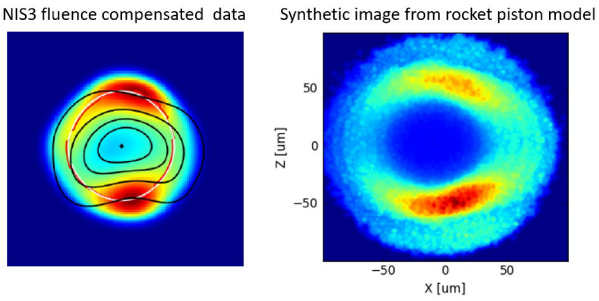

Figure 12: Measured fluence compensated down-scattered neutron image (a) compared to the synthetic image from the rocket-piston model (b). Note that the synthetic image shows low level scattering (a halo) outside the region of the data that may be beyond the signal-to-noise threshold of the measurement.

Figure 13 shows a comparison of all the synthetic image data from all current NIS lines-of-sight (many of which were not available on the shot and a few of which not currently available on the NIS2 instrument without significant upgrades). They show significant differences because of the 3D nature of the implosion. In particular, they show that a down-scattered image from the polar NIS2 image would show significant differences from the two equatorial images (NIS1 and NIS3) because of the presence of the ℓ=3 in the source flux asymmetry induced by the diagnostic windows.[45, 49] Also shown are synthetic gamma images from the carbon $^{12}C(n,n')^{*12}C$ reaction.[50, 51] The synthetic gamma images show significant structure from the assumed remaining HDC distribution that would be interesting attempt to observe with high resolution gamma images.[51]

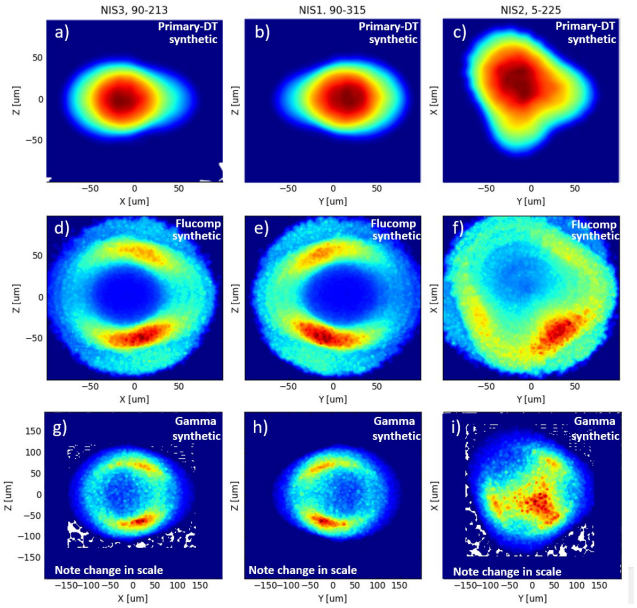

Figure 13: Gallery of synthetic images from each current neutron/gamma LOS from primary (a,b,c), fluence compensated down-scattered (d,e,f) and n,n' gamma (g,h,i) images. The gallery illustrates the full potential if each LOS could report the three images. Note that the NIS2 does not yet have an activate camera system and so cannot yet report the fluence compensated or gamma image.

Figure 14 shows the ρR_{WHM} plotted as the $1 - \rho R_{WHM}/\rho R_{AVG}$ as a function of time in the black curve along with the DT reaction rate as a function of time in red. As discussed in the introduction, the 6-piston model shows that the ρR_{WHM} is related to the residual kinetic energy and can be related to many of the performance degradations associated with 3D asymmetries.[10] Extracting the ρR_{WHM} from the available data for NIF implosions is a key motivation for the development of the rocket-piston model. The plot shows that the $1 - \rho R_{WHM}/\rho R_{AVG}$ grows substantially throughout the stagnation phase of the implosion and increases dramatically between minimum volume and peak burn. Therefore, the dynamics of this growth are important particularly for burning and igniting implosions that produce substantial yield and pressure after minimum volume.

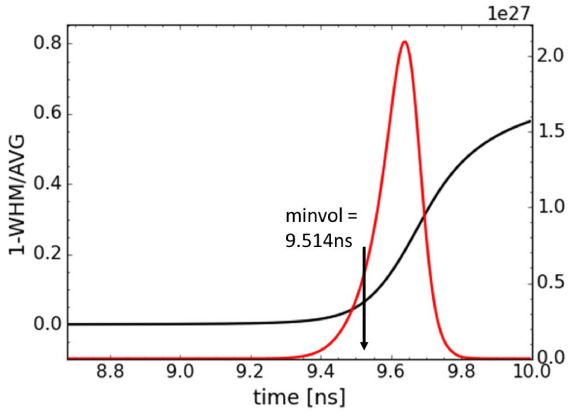

Figure 14: Dynamic plot of the asymmetry metric $f^2 = 1 - \rho R_{WHM}/\rho R_{AVG}$ estimated using the rocket-piston model as a function of time around minimum volume and bang-time (black curve) overlaid with the neutron emission (red curve).

The rocket-piston calculations shown in this section are not unique solutions but rather an example of the postshot capabilities that this model enables. Future work to rigorously fit the observables and explore uniqueness are now ongoing.[52]

IV. Summary

In summary, a rocket-piston model has been developed to study low-mode 3d asymmetries in NIF implosions. Low-mode asymmetries damage implosion performance by reducing the available energy that can be converted to hotspot internal energy and degrading the confinement of that energy. 3D asymmetries are diagnosed with the V_{HS}, RTNAD, primary x-ray and neutron images, and down-scattered neutron images. Currently, assembling a comprehensive picture of the implosion symmetry using high fidelity 3D radiation hydrodynamics simulations is impractical for every shot that is performed. This model is a computationally inexpensive capability that is designed to enable a host of post-shot capabilities where full 3D hydrodynamic simulations may not be practical.

The model has been applied to several recent shots of interest and the input perturbations required to match observations and indicate significant 3D asymmetries. Exploration of the uniqueness of the solutions that can match observations is an important question that will be explored with future work using Markov chain Monte Carlo and artificial intelligence techniques.[53] Likewise, we will explore how additional measurements (for example a third down-scattered imaging line-of-sight from the pole) will impact the uniqueness of forward fit solutions. Future studies will include carbon n,n′ gamma imaging in the reconstructions to attempt to understand asymmetries in ablator remaining mass and in ablator mix into the shell/hotspot.

Finally, the model can be used to infer the $\rho R_{WHM}/\rho R_{AVG}$, to make estimates of the residual kinetic energy, and understand impacts of observed asymmetries in diagnostic. The model itself solves the power balance equations which provide some estimate of the performance impact of perturbations as shown in Figure 7. Likewise, the model can be used with existing view-factor models to quickly forward model delivered laser power-balance asymmetries, with target metrology perturbations, to test consistency with observations and look for correlations with known seeds. Therefore, with knowledge of both impact and causes of asymmetries it may be possible to motivate future work to fix sources of asymmetry either by compensating using laser-power balance[54] or by eliminating the cause.

The authors sincerely thank the NIF operations staff who supported this work. This work was performed under the auspices of the U.S. Department of Energy by Lawrence Livermore National Laboratory under Contract DE-AC52-07NA27344. D. T. Casey acknowledges support from the U.S. Department of Energy Early Career Research Program through the Office of Fusion Energy Sciences.

References

1. H. Abu-Shawareb, R. Acree, P. Adams, J. Adams, B. Addis, R. Aden, P. Adrian, B. B. Afeyan, M. Aggleton, L. Aghaian, A. Aguirre, D. Aikens, J. Akre, F. Albert, M. Albrecht, B. J. Albright, J. Albritton, J. Alcala, C. Alday, D. A. Alessi, N. Alexander, J. Alfonso, N. Alfonso, E. Alger, S. J. Ali, Z. A. Ali, W. E. Alley, P. Amala, P. A. Amendt, P. Amick, S. Ammula, C. Amorin, D. J. Ampleford, R. W. Anderson, T. Anklam, N. Antipa, B. Appelbe, C. Aracne-Ruddle, E. Araya, M. Arend, P. Arnold, T. Arnold, J. Asay, L. J. Atherton, D. Atkinson, R. Atkinson, J. M. Auerbach, B. Austin, L. Auyang, A. S. Awwal, J. Ayers, S. Ayers, T. Ayers, S. Azevedo, B. Bachmann, C. A. Back, J. Bae, D. S. Bailey, J. Bailey, T. Baisden, K. L. Baker, H. Baldis, D. Barber, M. Barberis, D. Barker, A. Barnes, C. W. Barnes, M. A. Barrios, C. Barty, I. Bass, S. H. Batha, S. H. Baxamusa, G. Bazan, J. K. Beagle, R. Beale, B. R. Beck, J. B. Beck, M. Bedzyk, R. G. Beeler, R. G. Beeler, W. Behrendt, L. Belk, P. Bell, M. Belyaev, J. F. Benage, G. Bennett, L. R. Benedetti, L. X. Benedict, R. Berger, T. Bernat, L. A. Bernstein, B. Berry, L. Bertolini, G. Besenbruch, J. Betcher, R. Bettenhausen, R. Betti, B. Bezzerides, S. D. Bhandarkar, R. Bickel, J. Biener, T. Biesiada, K. Bigelow, J. Bigelow-Granillo, V. Bigman, R. M. Bionta, N. W. Birge, M. Bitter, A. C. Black, R. Bleile, D. L. Bleuel, E. Bliss, E. Bliss, B. Blue, T. Boehly, K. Boehm, C. D. Boley, R. Bonanno, E. J. Bond, T. Bond, M. J. Bonino, M. Borden, J. L. Bourgade, J. Bousquet, J. Bowers, M. Bowers, R. Boyd, A. Bozek, D. K. Bradley, K. S. Bradley, P. A. Bradley, L. Bradley, L. Brannon, P. S. Brantley, D. Braun, T. Braun, K. Brienza-Larsen, T. M. Briggs, J. Britten, E. D. Brooks, D. Browning, M. W. Bruhn, T. A. Brunner, H. Bruns, G. Brunton, B. Bryant, T. Buczek, J. Bude, L. Buitano, S. Burkhart, J. Burmark, A. Burnham, R. Burr, L. E. Busby, B. Butlin, R. Cabeltis, M. Cable, W. H. Cabot, B. Cagadas, J. Caggiano, R. Cahayag, S. E. Caldwell, S. Calkins, D. A. Callahan, J. Calleja-Aguirre, L. Camara, D. Camp, E. M. Campbell, J. H. Campbell, B. Carey, R. Carey, K. Carlisle, L. Carlson, L. Carman, J. Carmichael, A. Carpenter, C. Carr, J. A. Carrera, D. Casavant, A. Casey, D. T. Casey, A. Castillo, E. Castillo, J. I. Castor, C. Castro, W. Caughey, R. Cavitt, J. Celeste, P. M. Celliers, C. Cerjan, G. Chandler, B. Chang, C. Chang, J. Chang, L. Chang, R. Chapman, T. Chapman, L. Chase, H. Chen, H. Chen, K. Chen, L. Y. Chen, B. Cheng, J. Chittenden, C. Choate, J. Chou, R. E. Chrien, M. Chrisp, K. Christensen, M. Christensen, A. R. Christopherson, M. Chung, J. A. Church, A. Clark, D. S. Clark, K. Clark, R. Clark, L. Claus, B. Cline, J. A. Cline, J. A. Cobble, K. Cochrane, B. Cohen, S. Cohen, M. R. Collette, G. Collins, L. A. Collins, T. J. B. Collins, A. Conder, B. Conrad, M. Conyers, A. W. Cook, D. Cook, R. Cook, J. C. Cooley, G. Cooper, T. Cope, S. R. Copeland, F. Coppari, J. Cortez, J. Cox, D. H. Crandall, J. Crane, R. S. Craxton, M. Cray, A. Crilly, J. W. Crippen, D. Cross, M. Cuneo, G. Cuotts, C. E. Czajka, D. Czechowicz, T. Daly, P. Danforth, R. Darbee, B. Darlington, P. Datte, L. Dauffy, G. Davalos, S. Davidovits, P. Davis, J. Davis, S. Dawson, R. D. Day, T. H. Day, M. Dayton, C. Deck, C. Decker, C. Deeney, K. A. DeFriend, G. Deis, N. D. Delamater, J. A. Delettrez, R. Demaret, S. Demos, S. M. Dempsey, R. Desjardin, T. Desjardins, M. P. Desjarlais, E. L. Dewald, J. DeYoreo, S. Diaz, G. Dimonte, T. R. Dittrich, L. Divol, S. N. Dixit, J. Dixon, E. S. Dodd, D. Dolan, A. Donovan, M. Donovan, T. Döppner, C. Dorrer, N. Dorsano, M. R. Douglas, D. Dow, J. Downie, E. Downing, M. Dozieres, V. Draggoo, D. Drake, R. P. Drake, T. Drake, G. Dreifuerst, D. F. DuBois, P. F. DuBois, G. Dunham, R. Dylla-Spears, A. K. L. Dymoke-Bradshaw, B. Dzenitis, C. Ebbers, M. Eckart, S. Eddinger, D. Eder, D. Edgell, M. J. Edwards, P. Efthimion, J. H. Eggert, B. Ehrlich, P. Ehrmann, S. Elhadj, C. Ellerbee, N. S. Elliott, C. L. Ellison, F. Elsner, M. Emerich, K. Engelhorn, T. England, E. English, P. Epperson, R. Epstein, G. Erbert, M. A. Erickson, D. J. Erskine, A. Erlandson, R. J. Espinosa, C. Estes, K. G. Estabrook, S. Evans, A. Fabyan, J. Fair, R. Fallejo, N. Farmer, W. A. Farmer, M. Farrell, V. E. Fatherley, M. Fedorov, E. Feigenbaum, M. Feit, W. Ferguson, J. C. Fernandez, A. Fernandez-Panella, S. Fess, J. E. Field, C. V. Filip, J. R. Fincke, T. Finn, S. M. Finnegan, R. G. Finucane, M. Fischer, A. Fisher, J. Fisher, B. Fishler, D. Fittinghoff, P. Fitzsimmons, M. Flegel, K. A. Flippo, J. Florio, J. Folta, P. Folta, L. R. Foreman, C. Forrest, A. Forsman, J. Fooks, M. Foord, R. Fortner, K. Fournier, D. E. Fratanduono, N. Frazier, T. Frazier, C. Frederick, M. S. Freeman, J. Frenje, D. Frey, G. Frieders, S. Friedrich, D. H. Froula, J. Fry, T. Fuller, J. Gaffney, S. Gales, B. Le Galloudec, K. K. Le Galloudec, A. Gambhir, L. Gao, W. J. Garbett, A. Garcia, C. Gates, E. Gaut, P. Gauthier, Z. Gavin, J. Gaylord, M. Geissel, F. Génin, J. Georgeson, H. Geppert-Kleinrath, V. Geppert-Kleinrath, N. Gharibyan, J. Gibson, C. Gibson, E. Giraldez, V. Glebov, S. G. Glendinning, S. Glenn, S. H. Glenzer, S. Goade, P. L. Gobby, S. R. Goldman, B. Golick, M. Gomez, V. Goncharov, D. Goodin, P. Grabowski, E. Grafil, P. Graham, J. Grandy, E. Grasz, F. Graziani, G. Greenman, J. A. Greenough, A. Greenwood, G. Gregori, T. Green, J. R. Griego, G. P. Grim, J. Grondalski, S. Gross, J. Guckian, N. Guler, B. Gunney, G. Guss, S. Haan, J. Hackbarth, L. Hackel, R. Hackel, C. Haefner, C. Hagmann, K. D. Hahn, S. Hahn, B. J. Haid, B. M. Haines, B. M. Hall, C. Hall, G. N. Hall, M. Hamamoto, S. Hamel, C. E. Hamilton, B. A. Hammel, J. H. Hammer, G. Hampton, A. Hamza, A. Handler, S. Hansen, D. Hanson, R. Haque, D. Harding, E. Harding, J. D. Hares, D. B. Harris, J. A. Harte, E. P. Hartouni, R. Hatarik, S. Hatchett, A. A. Hauer, M. Havre, R. Hawley, J. Hayes, J. Hayes, S. Hayes, A. Hayes-Sterbenz, C. A. Haynam, D. A. Haynes, D. Headley, A. Heal, J. E. Heebner, S. Heerey, G. M. Heestand, R. Heeter, N. Hein, C. Heinbockel, C. Hendricks, M.

Henesian, J. Heninger, J. Henrikson, E. A. Henry, E. B. Herbold, M. R. Hermann, G. Hermes, J. E. Hernandez, V. J. Hernandez, M. C. Herrmann, H. W. Herrmann, O. D. Herrera, D. Hewett, R. Hibbard, D. G. Hicks, D. Hill, K. Hill, T. Hilsabeck, D. E. Hinkel, D. D. Ho, V. K. Ho, J. K. Hoffer, N. M. Hoffman, M. Hohenberger, M. Hohensee, W. Hoke, D. Holdener, F. Holdener, J. P. Holder, B. Holko, D. Holunga, J. F. Holzrichter, J. Honig, D. Hoover, D. Hopkins, L. Berzak Hopkins, M. Hoppe, M. L. Hoppe, J. Horner, R. Hornung, C. J. Horsfield, J. Horvath, D. Hotaling, R. House, L. Howell, W. W. Hsing, S. X. Hu, H. Huang, J. Huckins, H. Hui, K. D. Humbird, J. Hund, J. Hunt, O. A. Hurricane, M. Hutton, K. H. K. Huynh, L. Inandan, C. Iglesias, I. V. Igumenshchev, N. Izumi, M. Jackson, J. Jackson, S. D. Jacobs, G. James, K. Jancaitis, J. Jarboe, L. C. Jarrott, D. Jasion, J. Jaquez, J. Jeet, A. E. Jenei, J. Jensen, J. Jimenez, R. Jimenez, D. Jobe, Z. Johal, H. M. Johns, D. Johnson, M. A. Johnson, M. Gatu Johnson, R. J. Johnson, S. Johnson, S. A. Johnson, T. Johnson, K. Jones, O. Jones, M. Jones, R. Jorge, H. J. Jorgenson, M. Julian, B. I. Jun, R. Jungquist, J. Kaae, N. Kabadi, D. Kaczala, D. Kalantar, K. Kangas, V. V. Karasiev, M. Karasik, V. Karpenko, A. Kasarky, K. Kasper, R. Kauffman, M. I. Kaufman, C. Keane, L. Keaty, L. Kegelmeyer, P. A. Keiter, P. A. Kellett, J. Kellogg, J. H. Kelly, S. Kemic, A. J. Kemp, G. E. Kemp, G. D. Kerbel, D. Kershaw, S. M. Kerr, T. J. Kessler, M. H. Key, S. F. Khan, H. Khater, C. Kiikka, J. Kilkenny, Y. Kim, Y. J. Kim, J. Kimko, M. Kimmel, J. M. Kindel, J. King, R. K. Kirkwood, L. Klaus, D. Klem, J. L. Kline, J. Klingmann, G. Kluth, P. Knapp, J. Knauer, J. Knipping, M. Knudson, D. Kobs, J. Koch, T. Kohut, C. Kong, J. M. Koning, P. Koning, S. Konior, H. Kornblum, L. B. Kot, B. Kozioziemski, M. Kozlowski, P. M. Kozlowski, J. Krammen, N. S. Krasheninnikova, B. Kraus, W. Krauser, J. D. Kress, A. L. Kritcher, E. Krieger, J. J. Kroll, W. L. Kruer, M. K. G. Kruse, S. Kucheyev, M. Kumbera, S. Kumpan, J. Kunimune, B. Kustowski, T. J. T. Kwan, G. A. Kyrala, S. Laffite, M. Lafon, K. LaFortune, B. Lahmann, B. Lairson, O. L. Landen, J. Langenbrunner, L. Lagin, T. Land, M. Lane, D. Laney, A. B. Langdon, S. H. Langer, A. Langro, N. E. Lanier, T. E. Lanier, D. Larson, B. F. Lasinski, D. Lassle, D. LaTray, G. Lau, N. Lau, C. Laumann, A. Laurence, T. A. Laurence, J. Lawson, H. P. Le, R. R. Leach, L. Leal, A. Leatherland, K. LeChien, B. Lechleiter, A. Lee, M. Lee, T. Lee, R. J. Leeper, E. Lefebvre, J. P. Leidinger, B. LeMire, R. W. Lemke, N. C. Lemos, S. Le Pape, R. Lerche, S. Lerner, S. Letts, K. Levedahl, T. Lewis, C. K. Li, H. Li, J. Li, W. Liao, Z. M. Liao, D. Liedahl, J. Liebman, G. Lindford, E. L. Lindman, J. D. Lindl, H. Loey, R. A. London, F. Long, E. N. Loomis, F. E. Lopez, H. Lopez, E. Losbanos, S. Loucks, R. Lowe-Webb, E. Lundgren, A. P. Ludwigsen, R. Luo, J. Lusk, R. Lyons, T. Ma, Y. Macallop, M. J. MacDonald, B. J. MacGowan, J. M. Mack, A. J. Mackinnon, S. A. MacLaren, A. G. MacPhee, G. R. Magelssen, J. Magoon, R. M. Malone, T. Malsbury, R. Managan, R. Mancini, K. Manes, D. Maney, D. Manha, O. M. Mannion, A. M. Manuel, E. Mapoles, G. Mara, T. Marcotte, E. Marin, M. M. Marinak, C. Mariscal, D. A. Mariscal, E. F. Mariscal, E. V. Marley, J. A. Marozas, R. Marquez, C. D. Marshall, F. J. Marshall, M. Marshall, S. Marshall, J. Marticorena, D. Martinez, I. Maslennikov, D. Mason, R. J. Mason, L. Masse, W. Massey, P. E. Masson-Laborde, N. D. Masters, D. Mathisen, E. Mathison, J. Matone, M. J. Matthews, C. Mattoon, T. R. Mattsson, K. Matzen, C. W. Mauche, M. Mauldin, T. McAbee, M. McBurney, T. McCarville, R. L. McCrory, A. M. McEvoy, C. McGuffey, M. McInnis, P. McKenty, M. S. McKinley, J. B. McLeod, A. McPherson, B. McQuillan, M. Meamber, K. D. Meaney, N. B. Meezan, R. Meissner, T. A. Mehlhorn, N. C. Mehta, J. Menapace, F. E. Merrill, B. T. Merritt, E. C. Merritt, D. D. Meyerhofer, S. Mezyk, R. J. Mich, P. A. Michel, D. Milam, C. Miller, D. Miller, D. S. Miller, E. Miller, E. K. Miller, J. Miller, M. Miller, P. E. Miller, T. Miller, W. Miller, V. Miller-Kamm, M. Millot, J. L. Milovich, P. Minner, J. L. Miquel, S. Mitchell, K. Molvig, R. C. Montesanti, D. S. Montgomery, M. Monticelli, A. Montoya, J. D. Moody, A. S. Moore, E. Moore, M. Moran, J. C. Moreno, K. Moreno, B. E. Morgan, T. Morrow, J. W. Morton, E. Moses, K. Moy, R. Muir, M. S. Murillo, J. E. Murray, J. R. Murray, D. H. Munro, T. J. Murphy, F. M. Munteanu, J. Nafziger, T. Nagayama, S. R. Nagel, R. Nast, R. A. Negres, A. Nelson, D. Nelson, J. Nelson, S. Nelson, S. Nemethy, P. Neumayer, K. Newman, M. Newton, H. Nguyen, J. M. G. Di Nicola, P. Di Nicola, C. Niemann, A. Nikroo, P. M. Nilson, A. Nobile, V. Noorai, R. Nora, M. Norton, M. Nostrand, V. Note, S. Novell, P. F. Nowak, A. Nunez, R. A. Nyholm, M. O'Brien, A. Oceguera, J. A. Oertel, J. Okui, B. Olejniczak, J. Oliveira, P. Olsen, B. Olson, K. Olson, R. E. Olson, Y. P. Opachich, N. Orsi, C. D. Orth, M. Owen, S. Padalino, E. Padilla, R. Paguio, S. Paguio, J. Paisner, S. Pajoom, A. Pak, S. Palaniyappan, K. Palma, T. Pannell, F. Papp, D. Paras, T. Parham, H. S. Park, A. Pasternak, S. Patankar, M. V. Patel, P. K. Patel, R. Patterson, S. Patterson, B. Paul, M. Paul, E. Pauli, O. T. Pearce, J. Pearcy, B. Pedrotti, A. Peer, L. J. Pelz, B. Penetrante, J. Penner, A. Perez, L. J. Perkins, E. Pernice, T. S. Perry, S. Person, D. Petersen, T. Petersen, D. L. Peterson, E. B. Peterson, J. E. Peterson, J. L. Peterson, K. Peterson, R. R. Peterson, R. D. Petrasso, F. Philippe, T. J. Phipps, E. Piceno, Y. Ping, L. Pickworth, J. Pino, R. Plummer, G. D. Pollack, S. M. Pollaine, B. B. Pollock, D. Ponce, J. Ponce, J. Pontelandolfo, J. L. Porter, J. Post, O. Poujade, C. Powell, H. Powell, G. Power, M. Pozulp, M. Prantil, M. Prasad, S. Pratuch, S. Price, K. Primdahl, S. Prisbrey, R. Procassini, A. Pruyne, B. Pudliner, S. R. Qiu, K. Quan, M. Quinn, J. Quintenz, P. B. Radha, F. Rainer, J. E. Ralph, K. S. Raman, R. Raman, P. Rambo, S. Rana, A. Randewich, D. Rardin, M. Ratledge, N. Ravelo, F. Ravizza, M. Rayce, A. Raymond, B. Raymond, B. Reed, C. Reed, S. Regan, B. Reichelt, V. Reis, S. Reisdorf, V. Rekow, B. A. Remington, A. Rendon, W. Requieron, M. Rever, H. Reynolds, J. Reynolds, J. Rhodes, M. Rhodes, M. C. Richardson, B. Rice, N. G. Rice, R. Rieben, A. Rigatti, S. Riggs, H. G. Rinderknecht, K. Ring, B. Riordan, R. Riquier, C. Rivers, D. Roberts, V. Roberts, G. Robertson, H. F. Robey, J. Robles, P. Rocha, G. Rochau, J. Rodriguez, S. Rodriguez, M. Rosen, M. Rosenberg, G. Ross, J. S. Ross, P. Ross, J. Rouse, D. Rovang, A. M. Rubenchik, M. S. Rubery, C. L. Ruiz, M. Rushford, B. Russ, J. R. Rygg, B. S. Ryujin, R. A. Sacks, R. F. Sacks, K. Saito, T. Salmon, J. D. Salmonson, J. Sanchez, S. Samuelson, M. Sanchez, C. Sangster, A. Saroyan, J. Sater, A. Satsangi, S. Sauers, R. Saunders, J. P. Sauppe, R. Sawicki, D. Sayre, M. Scanlan, K. Schaffers, G. T. Schappert, S. Schiaffino, D. J. Schlossberg, D. W. Schmidt, M. J. Schmitt, D. H. G. Schneider, M. B. Schneider, R. Schneider, M. Schoff, M. Schollmeier, M. Schölmerich, C. R. Schroeder, S. E. Schrauth, H. A. Scott, I. Scott, J. M. Scott, R. H. H. Scott, C. R. Scullard, T. Sedillo, F. H. Seguin, W. Seka, J. Senecal, S. M. Sepke, L. Seppala, K. Sequoia, J. Severyn, J. M. Sevier, N. Sewell, S. Seznec, R. C. Shah, J. Shamlian, D. Shaughnessy, M. Shaw, R. Shaw, C. Shearer, R. Shelton, N. Shen, M. W. Sherlock, A. I. Shestakov, E. L. Shi, S. J. Shin, N. Shingleton, W. Shmayda, M. Shor, M. Shoup, C. Shuldberg, L. Siegel, F. J. Silva, A. N. Simakov, B. T. Sims, D. Sinars, P. Singh, H. Sio, K. Skulina, S. Skupsky, S. Slutz, M. Sluyter, V. A. Smalyuk, D. Smauley, R. M. Smeltser, C. Smith, I. Smith, J. Smith, L. Smith, R. Smith, R. Sohn, S. Sommer, C. Sorce, M. Sorem, J. M. Soures, M. L. Spaeth, B. K.

Spears, S. Speas, D. Speck, R. Speck, J. Spears, T. Spinka, P. T. Springer, M. Stadermann, B. Stahl, J. Stahoviak, L. G. Stanton, R. Steele, W. Steele, D. Steinman, R. Stemke, R. Stephens, S. Sterbenz, P. Sterne, D. Stevens, J. Stevers, C. B. Still, C. Stoeckl, W. Stoeffl, J. S. Stolken, C. Stolz, E. Storm, G. Stone, S. Stoupin, E. Stout, I. Stowers, R. Strauser, H. Streckart, J. Streit, D. J. Strozzi, T. Suratwala, G. Sutcliffe, L. J. Suter, S. B. Sutton, V. Svidzinski, G. Swadling, W. Sweet, A. Szoke, M. Tabak, M. Takagi, A. Tambazidis, V. Tang, M. Taranowski, L. A. Taylor, S. Telford, W. Theobald, M. Thi, A. Thomas, C. A. Thomas, I. Thomas, R. Thomas, I. J. Thompson, A. Thongstisubskul, C. B. Thorsness, G. Tietbohl, R. E. Tipton, M. Tobin, N. Tomlin, R. Tommasini, A. J. Toreja, J. Torres, R. P. J. Town, S. Townsend, J. Trenholme, A. Trivelpiece, C. Trosseille, H. Truax, D. Trummer, S. Trummer, T. Truong, D. Tubbs, E. R. Tubman, T. Tunnell, D. Turnbull, R. E. Turner, M. Ulitsky, R. Upadhye, J. L. Vaher, P. VanArsdall, D. VanBlarcom, M. Vandenboomgaerde, R. VanQuinlan, B. M. Van Wonterghem, W. S. Varnum, A. L. Velikovich, A. Vella, C. P. Verdon, B. Vermillion, S. Vernon, R. Vesey, J. Vickers, R. M. Vignes, M. Visosky, J. Vocke, P. L. Volegov, S. Vonhof, R. Von Rotz, H. X. Vu, M. Vu, D. Wall, J. Wall, R. Wallace, B. Wallin, D. Walmer, C. A. Walsh, C. F. Walters, C. Waltz, A. Wan, A. Wang, Y. Wang, J. S. Wark, B. E. Warner, J. Watson, R. G. Watt, P. Watts, J. Weaver, R. P. Weaver, S. Weaver, C. R. Weber, P. Weber, S. V. Weber, P. Wegner, B. Welday, L. Welser-Sherrill, K. Weiss, K. Widmann, G. F. Wheeler, W. Whistler, R. K. White, H. D. Whitley, P. Whitman, M. E. Wickett, C. Widmayer, J. Wiedwald, R. Wilcox, S. Wilcox, C. Wild, B. H. Wilde, C. H. Wilde, K. Wilhelmsen, M. D. Wilke, H. Wilkens, P. Wilkins, S. C. Wilks, E. A. Williams, G. J. Williams, W. Williams, W. H. Williams, D. C. Wilson, B. Wilson, E. Wilson, R. Wilson, S. Winters, J. Wisoff, M. Wittman, J. Wolfe, A. Wong, K. W. Wong, L. Wong, N. Wong, R. Wood, D. Woodhouse, J. Woodruff, D. T. Woods, S. Woods, B. N. Woodworth, E. Wooten, A. Wootton, K. Work, J. B. Workman, J. Wright, M. Wu, C. Wuest, F. J. Wysocki, H. Xu, M. Yamaguchi, B. Yang, S. T. Yang, J. Yatabe, C. B. Yeamans, B. C. Yee, S. A. Yi, L. Yin, B. Young, C. S. Young, C. V. Young, P. Young, K. Youngblood, R. Zacharias, G. Zagaris, N. Zaitseva, F. Zaka, F. Ze, B. Zeiger, M. Zika, G. B. Zimmerman, T. Zobrist, J. D. Zuegel, A. B. Zylstra and I. C. F. C. Indirect Drive, Physical Review Letters **129** (7), 075001 (2022).

2. E. I. Moses, Journal of Physics: Conference Series **112** (1), 012003 (2008).

3. I. C. F. C. The Indirect Drive, H. Abu-Shawareb, R. Acree, P. Adams, J. Adams, B. Addis, R. Aden, P. Adrian, B. B. Afeyan, M. Aggleton, L. Aghaian, A. Aguirre, D. Aikens, J. Akre, F. Albert, M. Albrecht, B. J. Albright, J. Albritton, J. Alcala, C. Alday, D. A. Alessi, N. Alexander, J. Alfonso, N. Alfonso, E. Alger, S. J. Ali, Z. A. Ali, A. Allen, W. E. Alley, P. Amala, P. A. Amendt, P. Amick, S. Ammula, C. Amorin, D. J. Ampleford, R. W. Anderson, T. Anklam, N. Antipa, B. Appelbe, C. Aracne-Ruddle, E. Araya, T. N. Archuleta, M. Arend, P. Arnold, T. Arnold, A. Arsenlis, J. Asay, L. J. Atherton, D. Atkinson, R. Atkinson, J. M. Auerbach, B. Austin, L. Auyang, A. A. S. Awwal, N. Aybar, J. Ayers, S. Ayers, T. Ayers, S. Azevedo, B. Bachmann, C. A. Back, J. Bae, D. S. Bailey, J. Bailey, T. Baisden, K. L. Baker, H. Baldis, D. Barber, M. Barberis, D. Barker, A. Barnes, C. W. Barnes, M. A. Barrios, C. Barty, I. Bass, S. H. Batha, S. H. Baxamusa, G. Bazan, J. K. Beagle, R. Beale, B. R. Beck, J. B. Beck, M. Bedzyk, R. G. Beeler, R. G. Beeler, W. Behrendt, L. Belk, P. Bell, M. Belyaev, J. F. Benage, G. Bennett, L. R. Benedetti, L. X. Benedict, R. L. Berger, T. Bernat, L. A. Bernstein, B. Berry, L. Bertolini, G. Besenbruch, J. Betcher, R. Bettenhausen, R. Betti, B. Bezzerides, S. D. Bhandarkar, R. Bickel, J. Biener, T. Biesiada, K. Bigelow, J. Bigelow-Granillo, V. Bigman, R. M. Bionta, N. W. Birge, M. Bitter, A. C. Black, R. Bleile, D. L. Bleuel, E. Bliss, E. Bliss, B. Blue, T. Boehly, K. Boehm, C. D. Boley, R. Bonanno, E. J. Bond, T. Bond, M. J. Bonino, M. Borden, J. L. Bourgade, J. Bousquet, J. Bowers, M. Bowers, R. Boyd, D. Boyle, A. Bozek, D. K. Bradley, K. S. Bradley, P. A. Bradley, L. Bradley, L. Brannon, P. S. Brantley, D. Braun, T. Braun, K. Brienza-Larsen, R. Briggs, T. M. Briggs, J. Britten, E. D. Brooks, D. Browning, M. W. Bruhn, T. A. Brunner, H. Bruns, G. Brunton, B. Bryant, T. Buczek, J. Bude, L. Buitano, S. Burkhart, J. Burmark, A. Burnham, R. Burr, L. E. Busby, B. Butlin, R. Cabeltis, M. Cable, W. H. Cabot, B. Cagadas, J. Caggiano, R. Cahayag, S. E. Caldwell, S. Calkins, D. A. Callahan, J. Calleja-Aguirre, L. Camara, D. Camp, E. M. Campbell, J. H. Campbell, B. Carey, R. Carey, K. Carlisle, L. Carlson, L. Carman, J. Carmichael, A. Carpenter, C. Carr, J. A. Carrera, D. Casavant, A. Casey, D. T. Casey, A. Castillo, E. Castillo, J. I. Castor, C. Castro, W. Caughey, R. Cavitt, J. Celeste, P. M. Celliers, C. Cerjan, G. Chandler, B. Chang, C. Chang, J. Chang, L. Chang, R. Chapman, T. D. Chapman, L. Chase, H. Chen, H. Chen, K. Chen, L. Y. Chen, B. Cheng, J. Chittenden, C. Choate, J. Chou, R. E. Chrien, M. Chrisp, K. Christensen, M. Christensen, N. S. Christiansen, A. R. Christopherson, M. Chung, J. A. Church, A. Clark, D. S. Clark, K. Clark, R. Clark, L. Claus, B. Cline, J. A. Cline, J. A. Cobble, K. Cochrane, B. Cohen, S. Cohen, M. R. Collette, G. W. Collins, L. A. Collins, T. J. B. Collins, A. Conder, B. Conrad, M. Conyers, A. W. Cook, D. Cook, R. Cook, J. C. Cooley, G. Cooper, T. Cope, S. R. Copeland, F. Coppari, J. Cortez, J. Cox, D. H. Crandall, J. Crane, R. S. Craxton, M. Cray, A. Crilly, J. W. Crippen, D. Cross, M. Cuneo, G. Cuotts, C. E. Czajka, D. Czechowicz, T. Daly, P. Danforth, C. Danly, R. Darbee, B. Darlington, P. Datte, L. Dauffy, G. Davalos, S. Davidovits, P. Davis, J. Davis, S. Dawson, R. D. Day, T. H. Day, M. Dayton, C. Deck, C. Decker, C. Deeney, K. A. DeFriend, G. Deis, N. D. Delamater, J. A. Delettrez, R. Demaret, S. Demos, S. M. Dempsey, R. Desjardin, T. Desjardins, M. P. Desjarlais, E. L. Dewald, J. DeYoreo, S. Diaz, G. Dimonte, T. R. Dittrich, L. Divol, S. N. Dixit, J. Dixon, A. Do, E. S. Dodd, D. Dolan, A. Donovan, M. Donovan, T. Döppner, C. Dorrer, N. Dorsano, M. R. Douglas, D. Dow, J. Downie, E. Downing, M. Dozieres, V. Draggoo, D. Drake, R. P. Drake, T. Drake, G. Dreifuerst, O. Drury, D. F. DuBois, P. F. DuBois, G. Dunham, M. Durocher, R. Dylla-Spears, A. K. L. Dymoke-Bradshaw, B. Dzenitis, C. Ebbers, M. Eckart, S. Eddinger, D. Eder, D. Edgell, M. J. Edwards, P. Efthimion, J. H. Eggert, B. Ehrlich, P. Ehrmann, S. Elhadj, C. Ellerbee, N. S. Elliott, C. L. Ellison, F. Elsner, M. Emerich, K. Engelhorn, T. England, E. English, P. Epperson, R. Epstein, G. Erbert, M. A. Erickson, D. J. Erskine, A. Erlandson, R. J. Espinosa, C. Estes, K. G. Estabrook, S. Evans, A. Fabyan, J. Fair, R. Fallejo, N. Farmer, W. A. Farmer, M. Farrell, V. E. Fatherley, M. Fedorov, E. Feigenbaum, T. Fehrenbach, M. Feit, B. Felker, W. Ferguson, J. C. Fernandez, A. Fernandez-Panella, S. Fess, J. E. Field, C. V. Filip, J. R. Fincke, T. Finn, S. M. Finnegan, R. G. Finucane, M. Fischer, A. Fisher, J. Fisher, B. Fishler, D. Fittinghoff, P. Fitzsimmons, M. Flegel, K. A. Flippo, J. Florio, J. Folta, P. Folta, L. R. Foreman, C. Forrest, A. Forsman, J. Fooks, M. Foord, R. Fortner, K. Fournier, D. E. Fratanduono, N. Frazier, T. Frazier, C. Frederick, M. S. Freeman, J. Frenje, D. Frey, G. Frieders, S. Friedrich, D. H. Froula, J. Fry, T. Fuller, J. Gaffney, S. Gales, B. Le Galloudec, K. K. Le Galloudec, A. Gambhir, L. Gao, W. J.

Garbett, A. Garcia, C. Gates, E. Gaut, P. Gauthier, Z. Gavin, J. Gaylord, C. G. R. Geddes, M. Geissel, F. Génin, J. Georgeson, H. Geppert-Kleinrath, V. Geppert-Kleinrath, N. Gharibyan, J. Gibson, C. Gibson, E. Giraldez, V. Glebov, S. G. Glendinning, S. Glenn, S. H. Glenzer, S. Goade, P. L. Gobby, S. R. Goldman, B. Golick, M. Gomez, V. Goncharov, D. Goodin, P. Grabowski, E. Grafil, P. Graham, J. Grandy, E. Grasz, F. R. Graziani, G. Greenman, J. A. Greenough, A. Greenwood, G. Gregori, T. Green, J. R. Griego, G. P. Grim, J. Grondalski, S. Gross, J. Guckian, N. Guler, B. Gunney, G. Guss, S. Haan, J. Hackbarth, L. Hackel, R. Hackel, C. Haefner, C. Hagmann, K. D. Hahn, S. Hahn, B. J. Haid, B. M. Haines, B. M. Hall, C. Hall, G. N. Hall, M. Hamamoto, S. Hamel, C. E. Hamilton, B. A. Hammel, J. H. Hammer, G. Hampton, A. Hamza, A. Handler, S. Hansen, D. Hanson, R. Haque, D. Harding, E. Harding, J. D. Hares, D. B. Harris, J. A. Harte, E. P. Hartouni, R. Hatarik, S. Hatchett, A. A. Hauer, M. Havre, R. Hawley, J. Hayes, J. Hayes, S. Hayes, A. Hayes-Sterbenz, C. A. Haynam, D. A. Haynes, D. Headley, A. Heal, J. E. Heebner, S. Heerey, G. M. Heestand, R. Heeter, N. Hein, C. Heinbockel, C. Hendricks, M. Henesian, J. Heninger, J. Henrikson, E. A. Henry, E. B. Herbold, M. R. Hermann, G. Hermes, J. E. Hernandez, V. J. Hernandez, M. C. Herrmann, H. W. Herrmann, O. D. Herrera, D. Hewett, R. Hibbard, D. G. Hicks, D. P. Higginson, D. Hill, K. Hill, T. Hilsabeck, D. E. Hinkel, D. D. Ho, V. K. Ho, J. K. Hoffer, N. M. Hoffman, M. Hohenberger, M. Hohensee, W. Hoke, D. Holdener, F. Holdener, J. P. Holder, B. Holko, D. Holunga, J. F. Holzrichter, J. Honig, D. Hoover, D. Hopkins, L. F. Berzak Hopkins, M. Hoppe, M. L. Hoppe, J. Horner, R. Hornung, C. J. Horsfield, J. Horvath, D. Hotaling, R. House, L. Howell, W. W. Hsing, S. X. Hu, H. Huang, J. Huckins, H. Hui, K. D. Humbird, J. Hund, J. Hunt, O. A. Hurricane, M. Hutton, K. H. K. Huynh, L. Inandan, C. Iglesias, I. V. Igumenshchev, I. Ivanovich, N. Izumi, M. Jackson, J. Jackson, S. D. Jacobs, G. James, K. Jancaitis, J. Jarboe, L. C. Jarrott, D. Jasion, J. Jaquez, J. Jeet, A. E. Jenei, J. Jensen, J. Jimenez, R. Jimenez, D. Jobe, Z. Johal, H. M. Johns, D. Johnson, M. A. Johnson, M. Gatu Johnson, R. J. Johnson, S. Johnson, S. A. Johnson, T. Johnson, K. Jones, O. Jones, M. Jones, R. Jorge, H. J. Jorgenson, M. Julian, B. I. Jun, R. Jungquist, J. Kaae, N. Kabadi, D. Kaczala, D. Kalantar, K. Kangas, V. V. Karasiev, M. Karasik, V. Karpenko, A. Kasarky, K. Kasper, R. Kauffman, M. I. Kaufman, C. Keane, L. Keaty, L. Kegelmeyer, P. A. Keiter, P. A. Kellett, J. Kellogg, J. H. Kelly, S. Kemic, A. J. Kemp, G. E. Kemp, G. D. Kerbel, D. Kershaw, S. M. Kerr, T. J. Kessler, M. H. Key, S. F. Khan, H. Khater, C. Kiikka, J. Kilkenny, Y. Kim, Y. J. Kim, J. Kimko, M. Kimmel, J. M. Kindel, J. King, R. K. Kirkwood, L. Klaus, D. Klem, J. L. Kline, J. Klingmann, G. Kluth, P. Knapp, J. Knauer, J. Knipping, M. Knudson, D. Kobs, J. Koch, T. Kohut, C. Kong, J. M. Koning, P. Koning, S. Konior, H. Kornblum, L. B. Kot, B. Kozioziemski, M. Kozlowski, P. M. Kozlowski, J. Krammen, N. S. Krasheninnikova, C. M. Krauland, B. Kraus, W. Krauser, J. D. Kress, A. L. Kritcher, E. Krieger, J. J. Kroll, W. L. Kruer, M. K. G. Kruse, S. Kucheyev, M. Kumbera, S. Kumpan, J. Kunimune, E. Kur, B. Kustowski, T. J. T. Kwan, G. A. Kyrala, S. Laffite, M. Lafon, K. LaFortune, L. Lagin, B. Lahmann, B. Lairson, O. L. Landen, T. Land, M. Lane, D. Laney, A. B. Langdon, J. Langenbrunner, S. H. Langer, A. Langro, N. E. Lanier, T. E. Lanier, D. Larson, B. F. Lasinski, D. Lassle, D. LaTray, G. Lau, N. Lau, C. Laumann, A. Laurence, T. A. Laurence, J. Lawson, H. P. Le, R. R. Leach, L. Leal, A. Leatherland, K. LeChien, B. Lechleiter, A. Lee, M. Lee, T. Lee, R. J. Leeper, E. Lefebvre, J. P. Leidinger, B. LeMire, R. W. Lemke, N. C. Lemos, S. Le Pape, R. Lerche, S. Lerner, S. Letts, K. Levedahl, T. Lewis, C. K. Li, H. Li, J. Li, W. Liao, Z. M. Liao, D. Liedahl, J. Liebman, G. Lindford, E. L. Lindman, J. D. Lindl, H. Loey, R. A. London, F. Long, E. N. Loomis, F. E. Lopez, H. Lopez, E. Losbanos, S. Loucks, R. Lowe-Webb, E. Lundgren, A. P. Ludwigsen, R. Luo, J. Lusk, R. Lyons, T. Ma, Y. Macallop, M. J. MacDonald, B. J. MacGowan, J. M. Mack, A. J. Mackinnon, S. A. MacLaren, A. G. MacPhee, G. R. Magelssen, J. Magoon, R. M. Malone, T. Malsbury, R. Managan, R. Mancini, K. Manes, D. Maney, D. Manha, O. M. Mannion, A. M. Manuel, M. J. E. Manuel, E. Mapoles, G. Mara, T. Marcotte, E. Marin, M. M. Marinak, D. A. Mariscal, E. F. Mariscal, E. V. Marley, J. A. Marozas, R. Marquez, C. D. Marshall, F. J. Marshall, M. Marshall, S. Marshall, J. Marticorena, J. I. Martinez, D. Martinez, I. Maslennikov, D. Mason, R. J. Mason, L. Masse, W. Massey, P. E. Masson-Laborde, N. D. Masters, D. Mathisen, E. Mathison, J. Matone, M. J. Matthews, C. Mattoon, T. R. Mattsson, K. Matzen, C. W. Mauche, M. Mauldin, T. McAbee, M. McBurney, T. McCarville, R. L. McCrory, A. M. McEvoy, C. McGuffey, M. McInnis, P. McKenty, M. S. McKinley, J. B. McLeod, A. McPherson, B. McQuillan, M. Meamber, K. D. Meaney, N. B. Meezan, R. Meissner, T. A. Mehlhorn, N. C. Mehta, J. Menapace, F. E. Merrill, B. T. Merritt, E. C. Merritt, D. D. Meyerhofer, S. Mezyk, R. J. Mich, P. A. Michel, D. Milam, C. Miller, D. Miller, D. S. Miller, E. Miller, E. K. Miller, J. Miller, M. Miller, P. E. Miller, T. Miller, W. Miller, V. Miller-Kamm, M. Millot, J. L. Milovich, P. Minner, J. L. Miquel, S. Mitchell, K. Molvig, R. C. Montesanti, D. S. Montgomery, M. Monticelli, A. Montoya, J. D. Moody, A. S. Moore, E. Moore, M. Moran, J. C. Moreno, K. Moreno, B. E. Morgan, T. Morrow, J. W. Morton, E. Moses, K. Moy, R. Muir, M. S. Murillo, J. E. Murray, J. R. Murray, D. H. Munro, T. J. Murphy, F. M. Munteanu, J. Nafziger, T. Nagayama, S. R. Nagel, R. Nast, R. A. Negres, A. Nelson, D. Nelson, J. Nelson, S. Nelson, S. Nemethy, P. Neumayer, K. Newman, M. Newton, H. Nguyen, J. M. G. Di Nicola, P. Di Nicola, C. Niemann, A. Nikroo, P. M. Nilson, A. Nobile, V. Noorai, R. C. Nora, M. Norton, M. Nostrand, V. Note, S. Novell, P. F. Nowak, A. Nunez, R. A. Nyholm, M. O'Brien, A. Oceguera, J. A. Oertel, A. L. Oesterle, J. Okui, B. Olejniczak, J. Oliveira, P. Olsen, B. Olson, K. Olson, R. E. Olson, Y. P. Opachich, N. Orsi, C. D. Orth, M. Owen, S. Padalino, E. Padilla, R. Paguio, S. Paguio, J. Paisner, S. Pajoom, A. Pak, S. Palaniyappan, K. Palma, T. Pannell, F. Papp, D. Paras, T. Parham, H. S. Park, A. Pasternak, S. Patankar, M. V. Patel, P. K. Patel, R. Patterson, S. Patterson, B. Paul, M. Paul, E. Pauli, O. T. Pearce, J. Pearcy, A. Pedretti, B. Pedrotti, A. Peer, L. J. Pelz, B. Penetrante, J. Penner, A. Perez, L. J. Perkins, E. Pernice, T. S. Perry, S. Person, D. Petersen, T. Petersen, D. L. Peterson, E. B. Peterson, J. E. Peterson, J. L. Peterson, K. Peterson, R. R. Peterson, R. D. Petrasso, F. Philippe, D. Phillion, T. J. Phipps, E. Piceno, L. Pickworth, Y. Ping, J. Pino, K. Piston, R. Plummer, G. D. Pollack, S. M. Pollaine, B. B. Pollock, D. Ponce, J. Ponce, J. Pontelandolfo, J. L. Porter, J. Post, O. Poujade, C. Powell, H. Powell, G. Power, M. Pozulp, M. Prantil, M. Prasad, S. Pratuch, S. Price, K. Primdahl, S. Prisbrey, R. Procassini, A. Pruyne, B. Pudliner, S. R. Qiu, K. Quan, M. Quinn, J. Quintenz, P. B. Radha, F. Rainer, J. E. Ralph, K. S. Raman, R. Raman, P. W. Rambo, S. Rana, A. Randewich, D. Rardin, M. Ratledge, N. Ravelo, F. Ravizza, M. Rayce, A. Raymond, B. Raymond, B. Reed, C. Reed, S. Regan, B. Reichelt, V. Reis, S. Reisdorf, V. Rekow, B. A. Remington, A. Rendon, W. Requieron, M. Rever, H. Reynolds, J. Reynolds, J. Rhodes, M. Rhodes, M. C. Richardson, B. Rice, N. G. Rice, R. Rieben, A. Rigatti, S. Riggs, H. G. Rinderknecht, K. Ring, B. Riordan, R. Riquier, C. Rivers, D. Roberts, V. Roberts, G.

Robertson, H. F. Robey, J. Robles, P. Rocha, G. Rochau, J. Rodriguez, S. Rodriguez, M. D. Rosen, M. Rosenberg, G. Ross, J. S. Ross, P. Ross, J. Rouse, D. Rovang, A. M. Rubenchik, M. S. Rubery, C. L. Ruiz, M. Rushford, B. Russ, J. R. Rygg, B. S. Ryujin, R. A. Sacks, R. F. Sacks, K. Saito, T. Salmon, J. D. Salmonson, J. Sanchez, S. Samuelson, M. Sanchez, C. Sangster, A. Saroyan, J. Sater, A. Satsangi, S. Sauers, R. Saunders, J. P. Sauppe, R. Sawicki, D. Sayre, M. Scanlan, K. Schaffers, G. T. Schappert, S. Schiaffino, D. J. Schlossberg, D. W. Schmidt, P. F. Schmit, J. M. Smidt, D. H. G. Schneider, M. B. Schneider, R. Schneider, M. Schoff, M. Schollmeier, C. R. Schroeder, S. E. Schrauth, H. A. Scott, I. Scott, J. M. Scott, R. H. H. Scott, C. R. Scullard, T. Sedillo, F. H. Seguin, W. Seka, J. Senecal, S. M. Sepke, L. Seppala, K. Sequoia, J. Severyn, J. M. Sevier, N. Sewell, S. Seznec, R. C. Shah, J. Shamlian, D. Shaughnessy, M. Shaw, R. Shaw, C. Shearer, R. Shelton, N. Shen, M. W. Sherlock, A. I. Shestakov, E. L. Shi, S. J. Shin, N. Shingleton, W. Shmayda, M. Shor, M. Shoup, C. Shuldberg, L. Siegel, F. J. Silva, A. N. Simakov, B. T. Sims, D. Sinars, P. Singh, H. Sio, K. Skulina, S. Skupsky, S. Slutz, M. Sluyter, V. A. Smalyuk, D. Smauley, R. M. Smeltser, C. Smith, I. Smith, J. Smith, L. Smith, R. Smith, R. Smith, M. Schölmerich, R. Sohn, S. Sommer, C. Sorce, M. Sorem, J. M. Soures, M. L. Spaeth, B. K. Spears, S. Speas, D. Speck, R. Speck, J. Spears, T. Spinka, P. T. Springer, M. Stadermann, B. Stahl, J. Stahoviak, J. Stanley, L. G. Stanton, R. Steele, W. Steele, D. Steinman, R. Stemke, R. Stephens, S. Sterbenz, P. Sterne, D. Stevens, J. Stevers, C. H. Still, C. Stoeckl, W. Stoeffl, J. S. Stolken, C. Stolz, E. Storm, G. Stone, S. Stoupin, E. Stout, I. Stowers, R. Strauser, H. Streckart, J. Streit, D. J. Strozzi, J. Stutz, L. Summers, T. Suratwala, G. Sutcliffe, L. J. Suter, S. B. Sutton, V. Svidzinski, G. Swadling, W. Sweet, A. Szoke, M. Tabak, M. Takagi, A. Tambazidis, V. Tang, M. Taranowski, L. A. Taylor, S. Telford, W. Theobald, M. Thi, A. Thomas, C. A. Thomas, I. Thomas, R. Thomas, I. J. Thompson, A. Thongstisubskul, C. B. Thorsness, G. Tietbohl, R. E. Tipton, M. Tobin, N. Tomlin, R. Tommasini, A. J. Toreja, J. Torres, R. P. J. Town, S. Townsend, J. Trenholme, A. Trivelpiece, C. Trosseille, H. Truax, D. Trummer, S. Trummer, T. Truong, D. Tubbs, E. R. Tubman, T. Tunnell, D. Turnbull, R. E. Turner, M. Ulitsky, R. Upadhye, J. L. Vaher, P. VanArsdall, D. VanBlarcom, M. Vandenboomgaerde, R. VanQuinlan, B. M. Van Wonterghem, W. S. Varnum, A. L. Velikovich, A. Vella, C. P. Verdon, B. Vermillion, S. Vernon, R. Vesey, J. Vickers, R. M. Vignes, M. Visosky, J. Vocke, P. L. Volegov, S. Vonhof, R. Von Rotz, H. X. Vu, M. Vu, D. Wall, J. Wall, R. Wallace, B. Wallin, D. Walmer, C. A. Walsh, C. F. Walters, C. Waltz, A. Wan, A. Wang, Y. Wang, J. S. Wark, B. E. Warner, J. Watson, R. G. Watt, P. Watts, J. Weaver, R. P. Weaver, S. Weaver, C. R. Weber, P. Weber, S. V. Weber, P. Wegner, B. Welday, L. Welser-Sherrill, K. Weiss, K. B. Wharton, G. F. Wheeler, W. Whistler, R. K. White, H. D. Whitley, P. Whitman, M. E. Wickett, K. Widmann, C. Widmayer, J. Wiedwald, R. Wilcox, S. Wilcox, C. Wild, B. H. Wilde, C. H. Wilde, K. Wilhelmsen, M. D. Wilke, H. Wilkens, P. Wilkins, S. C. Wilks, E. A. Williams, G. J. Williams, W. Williams, W. H. Williams, D. C. Wilson, B. Wilson, E. Wilson, R. Wilson, S. Winters, P. J. Wisoff, M. Wittman, J. Wolfe, A. Wong, K. W. Wong, L. Wong, N. Wong, R. Wood, D. Woodhouse, J. Woodruff, D. T. Woods, S. Woods, B. N. Woodworth, E. Wooten, A. Wootton, K. Work, J. B. Workman, J. Wright, M. Wu, C. Wuest, F. J. Wysocki, H. Xu, M. Yamaguchi, B. Yang, S. T. Yang, J. Yatabe, C. B. Yeamans, B. C. Yee, S. A. Yi, L. Yin, B. Young, C. S. Young, C. V. Young, P. Young, K. Youngblood, J. Yu, R. Zacharias, G. Zagaris, N. Zaitseva, F. Zaka, F. Ze, B. Zeiger, M. Zika, G. B. Zimmerman, T. Zobrist, J. D. Zuegel and A. B. Zylstra, Physical Review Letters **132** (6), 065102 (2024).

4. J. D. Lindl, P. Amendt, R. L. Berger, S. G. Glendinning, S. H. Glenzer, S. W. Haan, R. L. Kauffman, O. L. Landen and L. J. Suter, Physics of Plasmas **11**, 339 (2004).
5. S. Atzeni and J. Meyer-ter-Vehn, *The physics of inertial fusion*. (Oxford University Press, Oxford, 2004).
6. J. P. Freidberg, *Plasma physics and fusion energy*. (Cambridge University Press, Cambridge, 2007).
7. R. Betti, P. Y. Chang, B. K. Spears, K. S. Anderson, J. Edwards, M. Fatenejad, J. D. Lindl, R. L. McCrory, R. Nora and D. Shvarts, Physics of Plasmas **17** (5), 058102 (2010).
8. O. A. Hurricane, D. T. Casey, O. Landen, A. L. Kritcher, R. Nora, P. K. Patel, J. A. Gaffney, K. D. Humbird, J. E. Field, M. K. G. Kruse, J. L. Peterson and B. K. Spears, Physics of Plasmas **27** (6), 062704 (2020).
9. M. G. Johnson, D. T. Casey, J. A. Frenje, C.-K. Li, F. H. Seguin, R. D. Petrasso, R. Ashabranner, R. Bionta, S. LePape, M. McKernan, A. Mackinnon, J. D. Kilkenny, J. Knauer and T. C. Sangster, Physics of Plasmas **20** (4), 042707 (2013).
10. O. A. Hurricane, D. T. Casey, O. Landen, D. A. Callahan, R. Bionta, S. Haan, A. L. Kritcher, R. Nora, P. K. Patel, P. T. Springer and A. Zylstra, Physics of Plasmas **29** (1), 012703 (2022).
11. K. M. Woo and R. Betti, Physics of Plasmas **28** (5), 054503 (2021).
12. K. M. Woo and R. Betti, Physics of Plasmas **28** (5) (2021).
13. V. Gopalaswamy, R. Betti, P. B. Radha, A. J. Crilly, K. M. Woo, A. Lees, C. Thomas, I. V. Igumenshchev, S. C. Miller, J. P. Knauer, C. Stoeckl, C. J. Forrest, O. M. Mannion, Z. L. Mohamed, H. G. Rinderknecht and P. V. Heuer, Physics of Plasmas **29** (7), 072706 (2022).
14. C. J. Forrest, A. Crilly, A. Schwemmlein, M. Gatu-Johnson, O. M. Mannion, B. Appelbe, R. Betti, V. Y. Glebov, V. Gopalaswamy, J. P. Knauer, Z. L. Mohamed, P. B. Radha, S. P. Regan, C. Stoeckl and W. Theobald, Review of Scientific Instruments **93** (10) (2022).
15. F. E. Merrill, D. Bower, R. Buckles, D. D. Clark, C. R. Danly, O. B. Drury, J. M. Dzenitis, V. E. Fatherley, D. N. Fittinghoff, R. Gallegos, G. P. Grim, N. Guler, E. N. Loomis, S. Lutz, R. M. Malone, D. D. Martinson, D. Mares, D. J. Morley, G. L. Morgan, J. A. Oertel, I. L. Tregillis, P. L. Volegov, P. B. Weiss, C. H. Wilde and D. C. Wilson, Review of Scientific Instruments **83** (10), 10D317 (2012).
16. G. P. Grim, N. Guler, F. E. Merrill, G. L. Morgan, C. R. Danly, P. L. Volegov, C. H. Wilde, D. C. Wilson, D. S. Clark, D. E. Hinkel, O. S. Jones, K. S. Raman, N. Izumi, D. N. Fittinghoff, O. B. Drury, E. T. Alger, P. A. Arnold, R. C. Ashabranner, L. J. Atherton, M. A. Barrios, S. Batha, P. M. Bell, L. R. Benedetti, R. L. Berger, L. A. Bernstein, L. V. Berzins, R. Betti, S. D. Bhandarkar, R. M. Bionta, D. L. Bleuel, T. R. Boehly, E. J. Bond, M. W. Bowers, D. K. Bradley, G. K. Brunton, R. A. Buckles, S. C. Burkhart, R. F. Burr, J. A. Caggiano, D. A. Callahan, D. T. Casey, C. Castro, P. M. Celliers, C. J. Cerjan, G. A. Chandler, C. Choate, S. J. Cohen, G. W. Collins, G. W. Cooper, J. R. Cox, J. R. Cradick, P. S. Datte, E. L. Dewald, P. D. Nicola, J. M. D. Nicola, L. Divol, S. N. Dixit, R. Dylla-Spears, E. G. Dzenitis, M. J. Eckart, D. C. Eder, D. H. Edgell, M. J. Edwards, J. H. Eggert, R. B. Ehrlich, G. V. Erbert, J. Fair, D. R. Farley, B. Felker, R. J. Fortner, J. A. Frenje, G. Frieders, S. Friedrich, M. Gatu-Johnson, C. R. Gibson, E. Giraldez, V. Y. Glebov, S. M. Glenn, S. H. Glenzer, G.

Gururangan, S. W. Haan, K. D. Hahn, B. A. Hammel, A. V. Hamza, E. P. Hartouni, R. Hatarik, S. P. Hatchett, C. Haynam, M. R. Hermann, H. W. Herrmann, D. G. Hicks, J. P. Holder, D. M. Holunga, J. B. Horner, W. W. Hsing, H. Huang, M. C. Jackson, K. S. Jancaitis, D. H. Kalantar, R. L. Kauffman, M. I. Kauffman, S. F. Khan, J. D. Kilkenny, J. R. Kimbrough, R. Kirkwood, J. L. Kline, J. P. Knauer, K. M. Knittel, J. A. Koch, T. R. Kohut, B. J. Kozioziemski, K. Krauter, G. W. Krauter, A. L. Kritcher, J. Kroll, G. A. Kyrala, K. N. L. Fortune, G. LaCaille, L. J. Lagin, T. A. Land, O. L. Landen, D. W. Larson, D. A. Latray, R. J. Leeper, T. L. Lewis, S. LePape, J. D. Lindl, R. R. Lowe-Webb, T. Ma, B. J. MacGowan, A. J. MacKinnon, A. G. MacPhee, R. M. Malone, T. N. Malsbury, E. Mapoles, C. D. Marshall, D. G. Mathisen, P. McKenty, J. M. McNaney, N. B. Meezan, P. Michel, J. L. Milovich, J. D. Moody, A. S. Moore, M. J. Moran, K. Moreno, E. I. Moses, D. H. Munro, B. R. Nathan, A. J. Nelson, A. Nikroo, R. E. Olson, C. Orth, A. E. Pak, E. S. Palma, T. G. Parham, P. K. Patel, R. W. Patterson, R. D. Petrasso, R. Prasad, J. E. Ralph, S. P. Regan, H. Rinderknecht, H. F. Robey, G. F. Ross, C. L. Ruiz, F. H. Seguin, J. D. Salmonson, T. C. Sangster, J. D. Sater, R. L. Saunders, M. B. Schneider, D. H. Schneider, M. J. Shaw, N. Simanovskaia, B. K. Spears, P. T. Springer, C. Stoeckl, W. Stoeffl, L. J. Suter, C. A. Thomas, R. Tommasini, R. P. Town, A. J. Traille, B. V. Wonterghem, R. J. Wallace, S. Weaver, S. V. Weber, P. J. Wegner, P. K. Whitman, K. Widmann, C. C. Widmayer, R. D. Wood, B. K. Young, R. A. Zacharias and A. Zylstra, Physics of Plasmas **20** (5), 056320 (2013).

17. P. Volegov, C. R. Danly, D. N. Fittinghoff, G. P. Grim, N. Guler, N. Izumi, T. Ma, F. E. Merrill, A. L. Warrick, C. H. Wilde and D. C. Wilson, Review of Scientific Instruments **85** (2), 023508 (2014).

18. R. Hatarik, D. B. Sayre, J. A. Caggiano, T. Phillips, M. J. Eckart, E. J. Bond, C. Cerjan, G. P. Grim, E. P. Hartouni, J. P. Knauer, J. M. Mcnaney and D. H. Munro, Journal of Applied Physics **118** (18), 184502 (2015).

19. M. G. Johnson, J. A. Frenje, D. T. Casey, C. K. Li, F. H. Seguin, R. Petrasso, R. Ashabranner, R. M. Bionta, D. L. Bleuel, E. J. Bond, J. A. Caggiano, A. Carpenter, C. J. Cerjan, T. J. Clancy, T. Doeppner, M. J. Eckart, M. J. Edwards, S. Friedrich, S. H. Glenzer, S. W. Haan, E. P. Hartouni, R. Hatarik, S. P. Hatchett, O. S. Jones, G. Kyrala, S. L. Pape, R. A. Lerche, O. L. Landen, T. Ma, A. J. MacKinnon, M. A. McKernan, M. J. Moran, E. Moses, D. H. Munro, J. McNaney, H. S. Park, J. Ralph, B. Remington, J. R. Rygg, S. M. Sepke, V. Smalyuk, B. Spears, P. T. Springer, C. B. Yeamans, M. Farrell, D. Jasion, J. D. Kilkenny, A. Nikroo, R. Paguio, J. P. Knauer, V. Y. Glebov, T. C. Sangster, R. Betti, C. Stoeckl, J. Magoon, M. J. Shoup, III, G. P. Grim, J. Kline, G. L. Morgan, T. J. Murphy, R. J. Leeper, C. L. Ruiz, G. W. Cooper and A. J. Nelson, Review of Scientific Instruments **83** (10), 10D308 (2012).

20. O. M. Mannion, J. P. Knauer, V. Y. Glebov, C. J. Forrest, A. Liu, Z. L. Mohamed, M. H. Romanofsky, T. C. Sangster, C. Stoeckl and S. P. Regan, Nuclear Instruments and Methods in Physics Research Section A: Accelerators, Spectrometers, Detectors and Associated Equipment **964**, 163774 (2020).

21. J. A. Frenje, R. Bionta, E. J. Bond, J. A. Caggiano, D. T. Casey, C. Cerjan, J. Edwards, M. Eckart, D. N. Fittinghoff, S. Friedrich, V. Y. Glebov, S. Glenzer, G. Grim, S. Haan, R. Hatarik, S. Hatchett, M. G. Johnson, O. S. Jones, J. D. Kilkenny, J. P. Knauer, O. Landen, R. Leeper, S. L. Pape, R. Lerche, C. K. Li, A. Mackinnon, J. McNaney, F. E. Merrill, M. Moran, D. H. Munro, T. J. Murphy, R. D. Petrasso, R. Rygg, T. C. Sangster, F. H. Séguin, S. Sepke, B. Spears, P. Springer, C. Stoeckl and D. C. Wilson, Nuclear Fusion **53** (4), 043014 (2013).

22. C. B. Yeamans and D. L. Bleuel, Fusion Science and Technology **72** (2), 120-128 (2017).

23. C. Cerjan, P. T. Springer and S. M. Sepke, Physics of Plasmas (1994-present) **20** (5), 056319 (2013).

24. M. M. Marinak, G. D. Kerbel, N. A. Gentile, O. Jones, D. Munro, S. Pollaine, T. R. Dittrich and S. W. Haan, Physics of Plasmas **8** (5), 2275-2280 (2001).

25. J. A. Gaffney, S. T. Brandon, K. D. Humbird, M. K. G. Kruse, R. C. Nora, J. L. Peterson and B. K. Spears, Physics of Plasmas **26** (8) (2019).

26. R. Nora, J. E. Field, B. K. Spears, D. T. Casey, M. K. G. Kruse, D. A. Mariscal and P. Patel, Physics of Plasmas **27** (3), 032706 (2020).

27. P. T. Springer, O. A. Hurricane, J. H. Hammer, R. Betti, D. A. Callahan, E. M. Campbell, D. T. Casey, C. J. Cerjan, D. Cao, E. Dewald, L. Divol, T. Doeppner, M. J. Edwards, J. E. Field, C. Forrest, J. Frenje, J. A. Gaffney, M. Gatu-Johnson, V. Glebov, V. N. Goncharov, G. P. Grim, E. Hartouni, R. Hatarik, D. E. Hinkel, L. B. Hopkins, I. Igumenshchev, P. Knapp, J. P. Knauer, A. L. Kritcher, O. Landen, A. Pak, S. Le Pape, T. Ma, A. G. MacPhee, D. H. Munro, R. C. Nora, P. K. Patel, L. Peterson, P. B. Radha, S. P. Regan, H. Rinderknecht, C. Sangster, B. K. Spears and C. Stoeckl, Nuclear Fusion **59** (3) (2019).

28. D. T. Casey, B. J. MacGowan, J. D. Sater, A. B. Zylstra, O. L. Landen, J. Milovich, O. A. Hurricane, A. L. Kritcher, M. Hohenberger, K. Baker, S. Le Pape, T. Döppner, C. Weber, H. Huang, C. Kong, J. Biener, C. V. Young, S. Haan, R. C. Nora, S. Ross, H. Robey, M. Stadermann, A. Nikroo, D. A. Callahan, R. M. Bionta, K. D. Hahn, A. S. Moore, D. Schlossberg, M. Bruhn, K. Sequoia, N. Rice, M. Farrell and C. Wild, Physical Review Letters **126** (2), 025002 (2021).

29. R. E. Olson, G. A. Rochau, O. L. Landen and R. J. Leeper, Physics of Plasmas **18** (3), 032706 (2011).

30. P. Amendt, A. I. Shestakov, O. L. Landen, D. K. Bradley, S. M. Pollaine, L. J. Suter and R. E. Turner, Physics of Plasmas **8** (6), 2908-2917 (2001).

31. O. A. Hurricane, D. A. Callahan, D. T. Casey, E. L. Dewald, T. R. Dittrich, T. Doppner, S. Haan, D. E. Hinkel, L. F. Berzak Hopkins, O. Jones, A. L. Kritcher, S. Le Pape, T. Ma, A. G. MacPhee, J. L. Milovich, J. Moody, A. Pak, H. S. Park, P. K. Patel, J. E. Ralph, H. F. Robey, J. S. Ross, J. D. Salmonson, B. K. Spears, P. T. Springer, R. Tommasini, F. Albert, L. R. Benedetti, R. Bionta, E. Bond, D. K. Bradley, J. Caggiano, P. M. Celliers, C. Cerjan, J. A. Church, R. Dylla-Spears, D. Edgell, M. J. Edwards, D. Fittinghoff, M. A. Barrios Garcia, A. Hamza, R. Hatarik, H. Herrmann, M. Hohenberger, D. Hoover, J. L. Kline, G. Kyrala, B. Kozioziemski, G. Grim, J. E. Field, J. Frenje, N. Izumi, M. Gatu Johnson, S. F. Khan, J. Knauer, T. Kohut, O. Landen, F. Merrill, P. Michel, A. Moore, S. R. Nagel, A. Nikroo, T. Parham, R. R. Rygg, D. Sayre, M. Schneider, D. Shaughnessy, D. Strozzi, R. P. J. Town, D. Turnbull, P. Volegov, A. Wan, K. Widmann, C. Wilde and C. Yeamans, Nat Phys **12**, 800-806 (2016).

32. D. A. Callahan, O. A. Hurricane, A. L. Kritcher, D. T. Casey, D. E. Hinkel, Y. P. Opachich, H. F. Robey, M. D. Rosen, J. S. Ross, M. S. Rubery, C. V. Young and A. B. Zylstra, Physics of Plasmas **27** (7), 072704 (2020).

33. M. J. May, J. R. Patterson, C. Sorce, K. Widmann, K. B. Fournier and F. Perez, Review of Scientific Instruments **83** (10), 10E117 (2012).

34. E. L. Dewald, K. M. Campbell, R. E. Turner, J. P. Holder, O. L. Landen, S. H. Glenzer, R. L. Kauffman, L. J. Suter, M. Landon, M. Rhodes and D. Lee, Review of Scientific Instruments **75** (10), 3759-3761 (2004).
35. O. A. Hurricane, D. A. Callahan, P. T. Springer, M. J. Edwards, P. Patel, K. Baker, D. T. Casey, L. Divol, T. Doppner, D. E. Hinkel, L. F. B. Hopkins, A. Kritcher, S. Le Pape, S. Maclaren, L. Masse, A. Pak, L. Pickworth, J. Ralph, C. Thomas, A. Yi and A. Zylstra, Plasma Physics and Controlled Fusion **61** (1) (2019).
36. A. L. Kritcher, R. Town, D. Bradley, D. Clark, B. Spears, O. Jones, S. Haan, P. T. Springer, J. Lindl, R. H. H. Scott, D. Callahan, M. J. Edwards and O. L. Landen, Physics of Plasmas **21** (4), 042708 (2014).
37. J. D. Lindl, S. W. Haan, O. L. Landen, A. R. Christopherson and R. Betti, Physics of Plasmas **25** (12), 122704 (2018).
38. F. B. Brown, R. F. Barrett, T. E. Booth, J. S. Bull, L. J. Cox, R. A. Forster, T. J. Goorley, R. D. Mosteller, S. E. Post, R. E. Prael, E. C. Selcow, A. Sood and J. Sweezy, Transactions of the American Nuclear Society **87**, 273 (2002).
39. D. T. Casey, P. L. Volegov, F. E. Merrill, D. H. Munro, G. P. Grim, O. L. Landen, B. K. Spears, D. N. Fittinghoff, J. E. Field and V. A. Smalyuk, Review of Scientific Instruments **87** (11), 11E715 (2016).
40. L. B. Hopkins, S. LePape, L. Divol, A. Pak, E. Dewald, D. D. Ho, N. Meezan, S. Bhandarkar, L. R. Benedetti, T. Bunn, J. Biener, J. Crippen, D. Casey, D. Clark, D. Edgell, D. Fittinghoff, M. Gatu-Johnson, C. Goyon, S. Haan, R. Hatarik, M. Havre, D. Hinkel, H. Huang, N. Izumi, J. Jaquez, O. Jones, S. Khan, A. Kritcher, C. Kong, G. Kyrala, O. Landen, T. Ma, A. MacPhee, B. MacGowan, A. J. Mackinnon, M. Marinak, J. Milovich, M. Millot, P. Michel, A. Moore, S. R. Nagel, A. Nikroo, P. Patel, J. Ralph, H. Robey, J. S. Ross, N. G. Rice, S. Sepke, V. A. Smalyuk, P. Sterne, D. Strozzi, M. Stadermann, P. Volegov, C. Weber, C. Wild, C. Yeamans, D. Callahan, O. Hurricane, R. P. J. Town and M. J. Edwards, Plasma Physics and Controlled Fusion **61** (1), 014023 (2018).
41. D. T. Casey, O. L. Landen, E. Hartouni, R. M. Bionta, K. D. Hahn, P. L. Volegov, D. N. Fittinghoff, V. Geppert-Kleinrath, C. H. Wilde, J. L. Milovich, V. A. Smalyuk, J. E. Field, O. A. Hurricane, A. B. Zylstra, A. L. Kritcher, D. S. Clark, C. V. Young, R. C. Nora, D. A. Callahan, B. J. MacGowan, D. H. Munro, B. K. Spears, J. L. Peterson, J. A. Gaffney, K. D. Humbird, M. K. G. Kruse, A. S. Moore, D. J. Schlossberg, M. Gatu-Johnson and J. A. Frenje, Physics of Plasmas **28** (4), 11 (2021).
42. A. S. Moore, D. J. Schlossberg, E. P. Hartouni, D. Sayre, M. J. Eckart, R. Hatarik, F. Barbosa, J. Root, C. Waltz, B. Beeman, M. S. Rubery and G. P. Grim, Review of Scientific Instruments **89** (10), 10I120 (2018).
43. A. L. Kritcher, A. B. Zylstra, C. R. Weber, O. A. Hurricane, D. A. Callahan, D. S. Clark, L. Divol, D. E. Hinkel, K. Humbird, O. Jones, J. D. Lindl, S. Maclaren, D. J. Strozzi, C. V. Young, A. Allen, B. Bachmann, K. L. Baker, T. Braun, G. Brunton, D. T. Casey, T. Chapman, C. Choate, E. Dewald, J. M. G. Di Nicola, M. J. Edwards, S. Haan, T. Fehrenbach, M. Hohenberger, E. Kur, B. Kustowski, C. Kong, O. L. Landen, D. Larson, B. J. MacGowan, M. Marinak, M. Millot, A. Nikroo, R. Nora, A. Pak, P. K. Patel, J. E. Ralph, M. Ratledge, M. S. Rubery, D. J. Schlossberg, S. M. Sepke, M. Stadermann, T. I. Suratwala, R. Tommasini, R. Town, B. Woodworth, B. Van Wonterghem and C. Wild, Physical Review E **109** (2), 025204 (2024).
44. A. Pak, A. B. Zylstra, K. L. Baker, D. T. Casey, E. Dewald, L. Divol, M. Hohenberger, A. S. Moore, J. E. Ralph, D. J. Schlossberg, R. Tommasini, N. Aybar, B. Bachmann, R. M. Bionta, D. Fittinghoff, M. Gatu Johnson, H. Geppert Kleinrath, V. Geppert Kleinrath, K. D. Hahn, M. S. Rubery, O. L. Landen, J. D. Moody, L. Aghaian, A. Allen, S. H. Baxamusa, S. D. Bhandarkar, J. Biener, N. W. Birge, T. Braun, T. M. Briggs, C. Choate, D. S. Clark, J. W. Crippen, C. Danly, T. Döppner, M. Durocher, M. Erickson, T. Fehrenbach, M. Freeman, M. Havre, S. Hayes, T. Hilsabeck, J. P. Holder, K. D. Humbird, O. A. Hurricane, N. Izumi, S. M. Kerr, S. F. Khan, Y. H. Kim, C. Kong, J. Jeet, B. Kozioziemski, A. L. Kritcher, K. M. Lamb, N. C. Lemos, B. J. MacGowan, A. J. Mackinnon, A. G. MacPhee, E. V. Marley, K. Meaney, M. Millot, J. M. G. Di Nicola, A. Nikroo, R. Nora, M. Ratledge, J. S. Ross, S. J. Shin, V. A. Smalyuk, M. Stadermann, S. Stoupin, T. Suratwala, C. Trosseille, B. Van Wonterghem, C. R. Weber, C. Wild, C. Wilde, P. T. Wooddy, B. N. Woodworth and C. V. Young, Physical Review E **109** (2), 025203 (2024).
45. B. J. MacGowan, O. L. Landen, D. T. Casey, C. V. Young, D. A. Callahan, E. P. Hartouni, R. Hatarik, M. Hohenberger, T. Ma, D. Mariscal, A. Moore, R. Nora, H. G. Rinderknecht, D. Schlossberg and B. M. Van Wonterghem, High Energy Density Physics **40**, 100944 (2021).
46. M. Gatu Johnson, J. A. Frenje, R. M. Bionta, D. T. Casey, M. J. Eckart, M. P. Farrell, G. P. Grim, E. P. Hartouni, R. Hatarik, M. Hoppe, J. D. Kilkenny, C. K. Li, R. D. Petrasso, H. G. Reynolds, D. B. Sayre, M. E. Schoff, F. H. Séguin, K. Skulina and C. B. Yeamans, Review of Scientific Instruments **87** (11), 11D816 (2016).
47. D. Casey, B. MacGowan, O. Hurricane, O. Landen, R. Nora, S. Haan, A. Kritcher, A. Zylstra, J. Ralph, E. Dewald, M. Hohenberger, A. Pak, P. Springer, C. Weber, J. Milovich, L. Divol, E. Hartouni, R. Bionta, K. Hahn, D. Schlossberg, A. Moore and M. Gatu Johnson, Physical Review E **108** (5), L053203 (2023).
48. R. C. Nora, N. Birge, D. Casey, C. Danly, E. L. Dewald, B. Z. Djordjevic, A. Do, M. Durocher, J. E. Field, D. Fittinghoff, M. S. Freeman, J. Gaffney, V. Geppert Kleinrath, S. Haan, K. Hahn, E. Hartouni, M. Hohenberger, S. Kerr, O. L. Landen, J. Milovich, A. S. Moore, P. Patel, D. J. Schlossberg, S. M. Sepke, B. K. Spears, P. L. Volegov and C. Wilde, Physics of Plasmas **30** (9) (2023).
49. J. L. Milovich, D. C. Casey, B. MacGowan, D. Clark, D. Mariscal, T. Ma, K. Baker, R. Bionta, K. Hahn, A. Moore, D. Schlossberg, E. Hartouni, S. Sepke and O. Landen, Plasma Physics and Controlled Fusion **63** (2), 025012 (2020).
50. V. Geppert-Kleinrath, N. Hoffman, N. Birge, A. DeYoung, D. Fittinghoff, M. Freeman, H. Geppert-Kleinrath, Y. Kim, K. Meaney, G. Morgan, M. Rubery, L. Tafoya, C. Wilde and P. Volegov, Physics of Plasmas **30** (2) (2023).
51. M. Rubery, D. Fittinghoff, N. Cherepy, C. Danly, V. Geppert-Kleinrath, V. Fatherley, H. Jorgenson, M. Freeman, C. Wilde, P. Volegov, M. Durocher, G. Saavedra, A. Moore, D. Schlossberg, E. Casco, S. Payne, R. Osborne, Z. Seeley, C. McNamee and C. Waltz, *Improved gamma imaging at NIF using the ceramic scintillator GYGAG*. (SPIE, 2023).
52. Kuminume private communciation. J. Kunimune et al., submited to rev. sci. instrum.
53. J. Kunimune et al., private communication.
54. O. M. Mannion, I. V. Igumenshchev, K. S. Anderson, R. Betti, E. M. Campbell, D. Cao, C. J. Forrest, M. G. Johnson, V. Y. Glebov, V. N. Goncharov, V. Gopalaswamy, S. T. Ivancic, D. W. Jacobs-Perkins, A. Kalb, J. P. Knauer, J. Kwiatkowski, A. Lees, F.

J. Marshall, M. Michalko, Z. L. Mohamed, D. Patel, H. G. Rinderknecht, R. C. Shah, C. Stoeckl, W. Theobald, K. M. Woo and S. P. Regan, Physics of Plasmas **28** (4), 042701 (2021).